Imperial College London

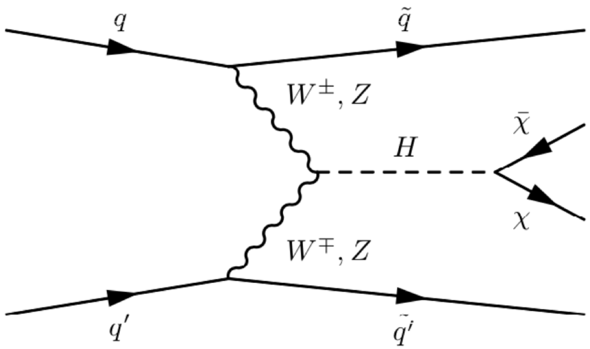

Higgs-to-Invisible Searches with the CMS experiment at the LHC

Riccardo Di Maria

Imperial College London
riccardo.di.maria@cern.ch

Joint APP and HEPP Annual Conference, 27 March 2018, University of Bristol (UK)

Contents

- Introduction and Motivation
- Physics Background
- VBF Higgs-to-Invisible Search
- Combination
- Dark Matter Interpretation
- Conclusions

Motivation

- Strong astrophysical evidence indicates that dark matter (DM) exists.

- There is no evidence yet for non-gravitational interactions between DM and standard model (SM) particles.

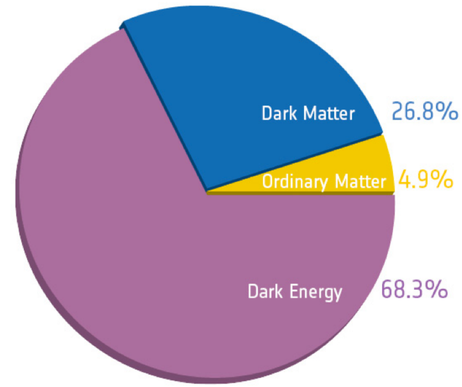

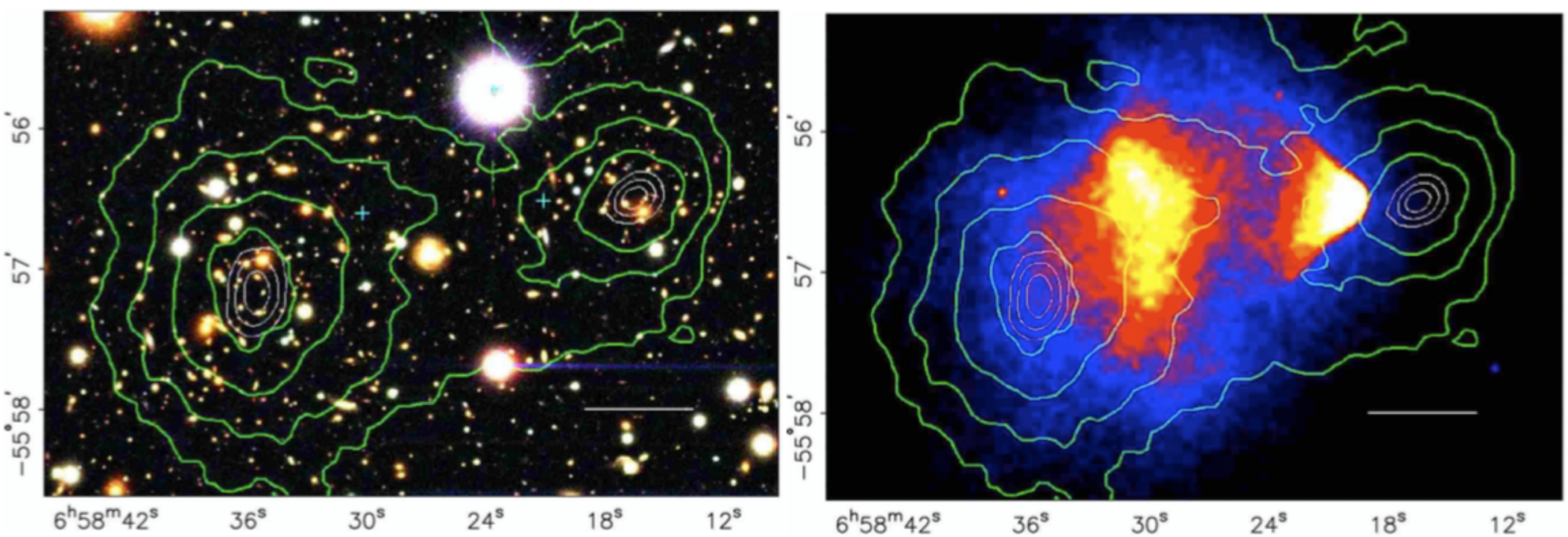

arXiv:astro-ph/0608407

- The LHC provides an opportunity to probe these interactions by directly producing DM particles.

Why Higgs to Invisible?

- Higgs boson decays to invisible final states predicted by many beyond the SM (BSM) theories, where final state particles can be DM candidates.

- The Higgs boson (125 GeV) measurements are compatible with the SM expectation.
- However, present uncertainties can accommodate BSM properties.
- BSM Higgs decays affect the total Higgs boson width.
- The SM branching ratio H(inv.) is ≈0.12% for H(ZZ(4ν)).
- Invisibly decaying Higgs boson is a hint of new physics.

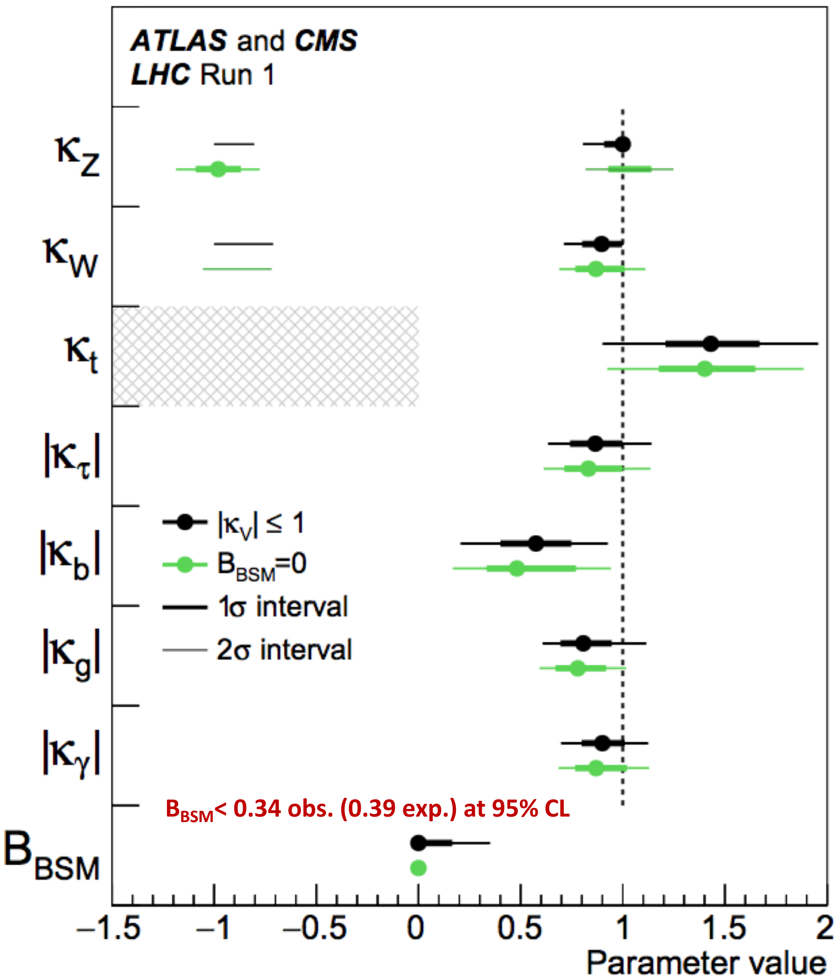

arXiv.: 1606.02266

Direct Searches

- Higgs boson has to recoil against a visible system.

vector boson fusion (qqH)

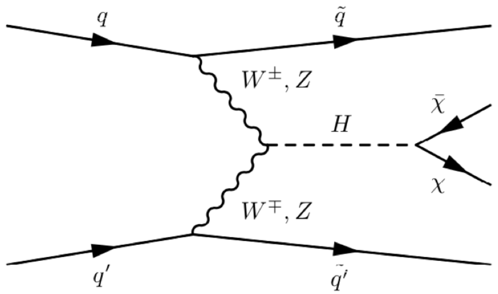

- Missing transverse energy (MET) has to be present in the final state.

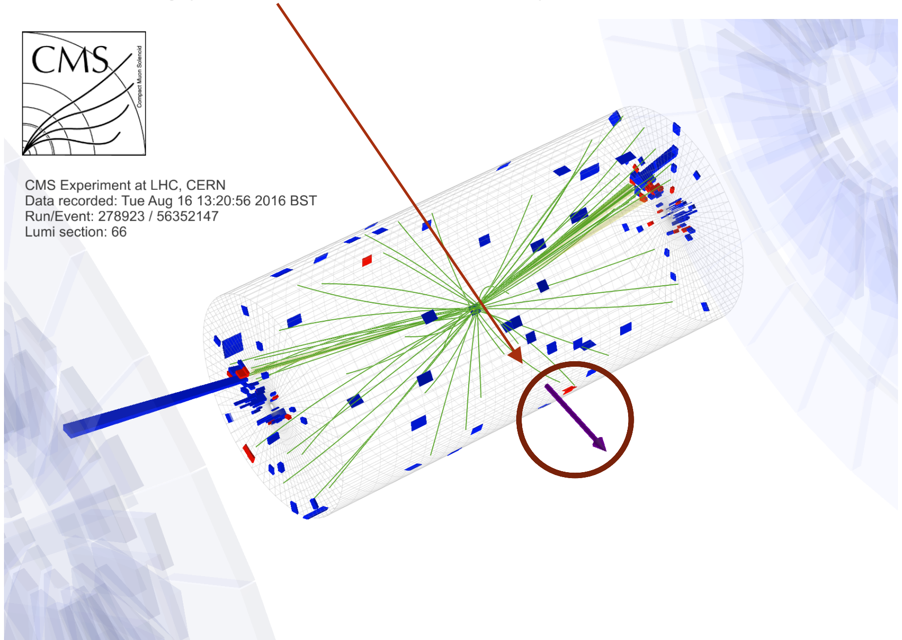

VBF H(inv.)

- The final state is characterised by:
  2 jets with large $\Delta\eta_{jj}$; large m_{jj}; large MET well-separated from any jets.

- Expected backgrounds:
  Z(νν)+jets; W(ℓν)+jets, where ℓ is missed;
  Top quark, diboson, and QCD multijet.

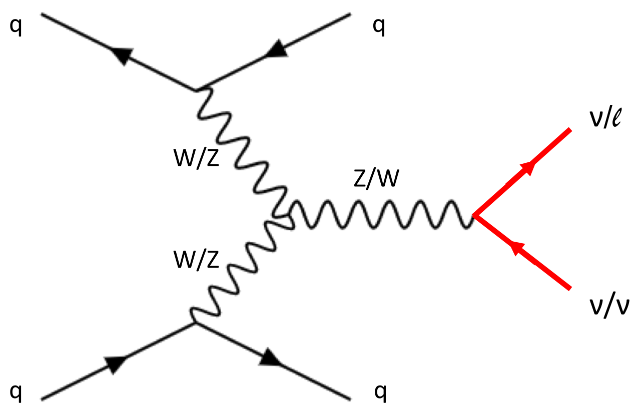

- Two different approaches used:
  - *cut-and-count*, results directly translated into a limit on the visible cross-section in a model independent way;
  - *shape*, improves the sensitivity for a SM-like H(inv.).

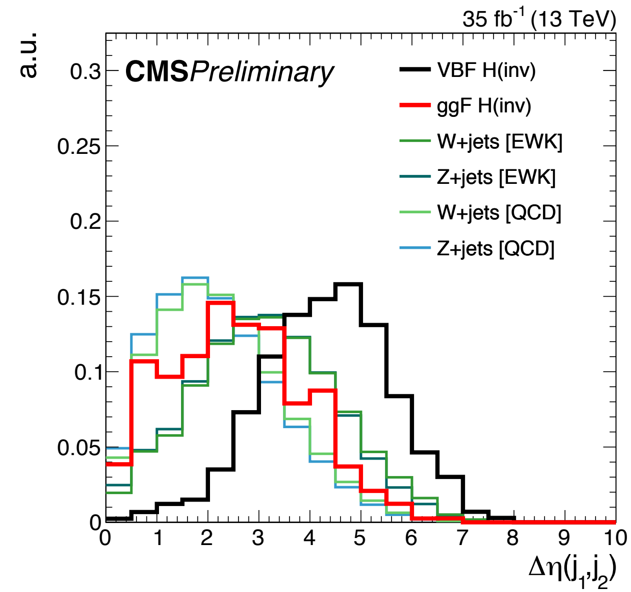

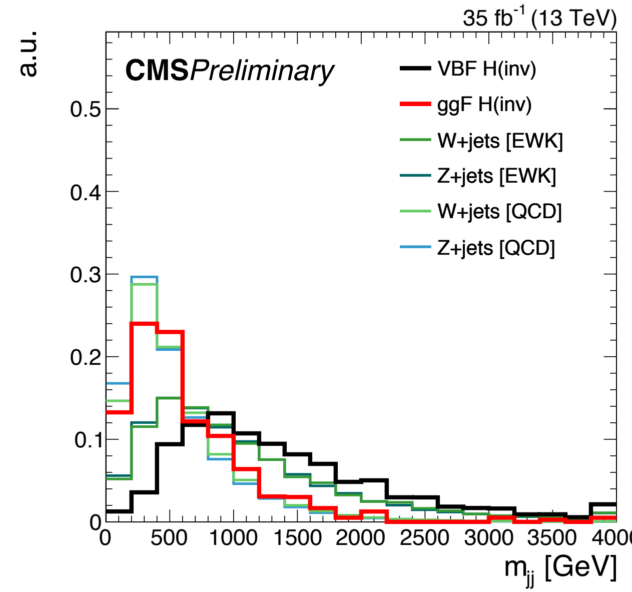

Control Regions

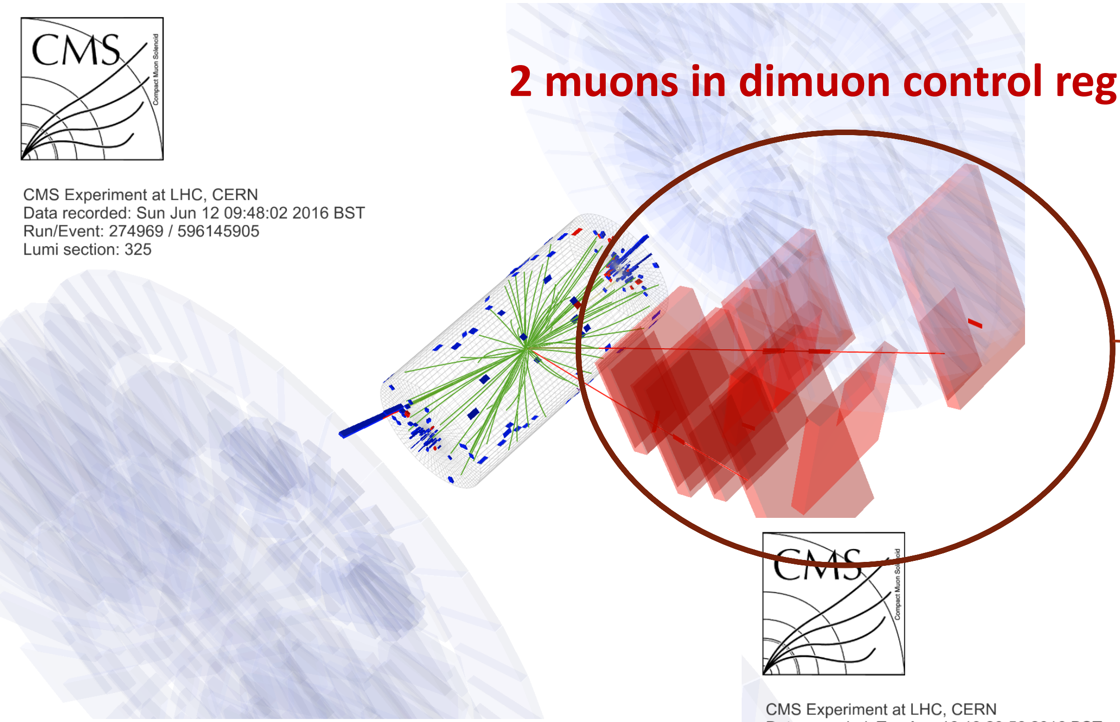

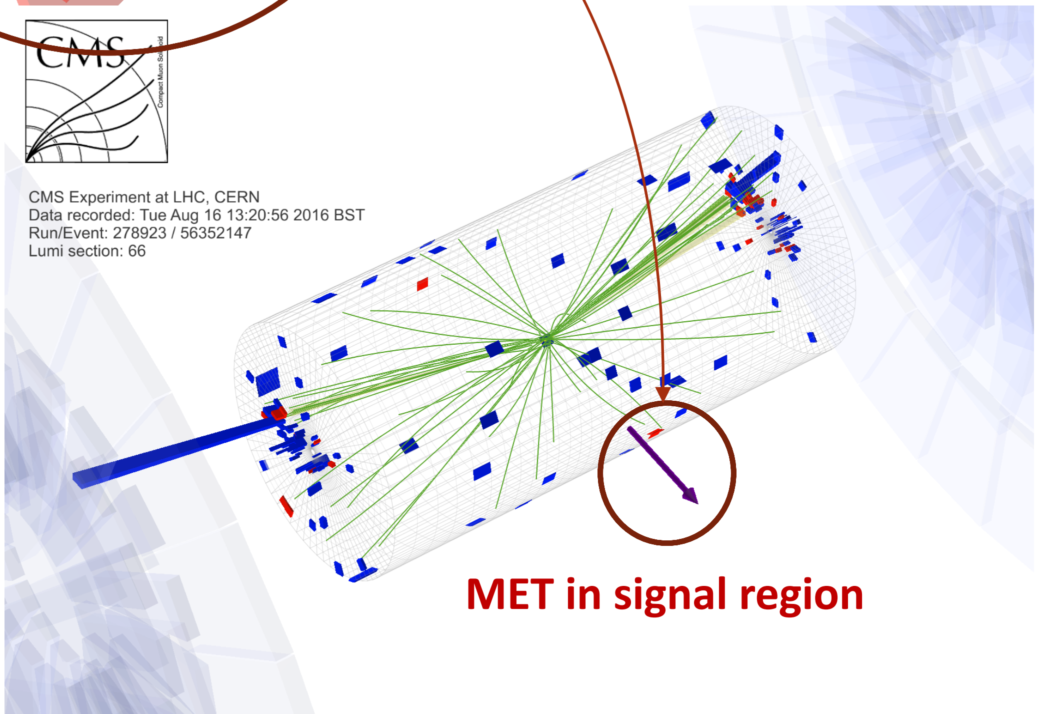

- The V+jets represent the largest backgrounds in this search (≈95%), and are determined through a simultaneous maximum-likelihood fit across 4 CRs and SR.

Muon CRs

- Events selected using the same SR $p_T^{miss}{}_{trig}$.

- 2 oppositely charged μ with p_T > 10 GeV:
  - at least one with p_T > 20 GeV that passes tighter ID;
  - 60 < $m_{\mu\mu}$ < 120 GeV.

- 1 μ with p_T > 20 GeV, passing both tight ID and ISO requirements.
- m_T < 160 GeV for the muon-MET system.

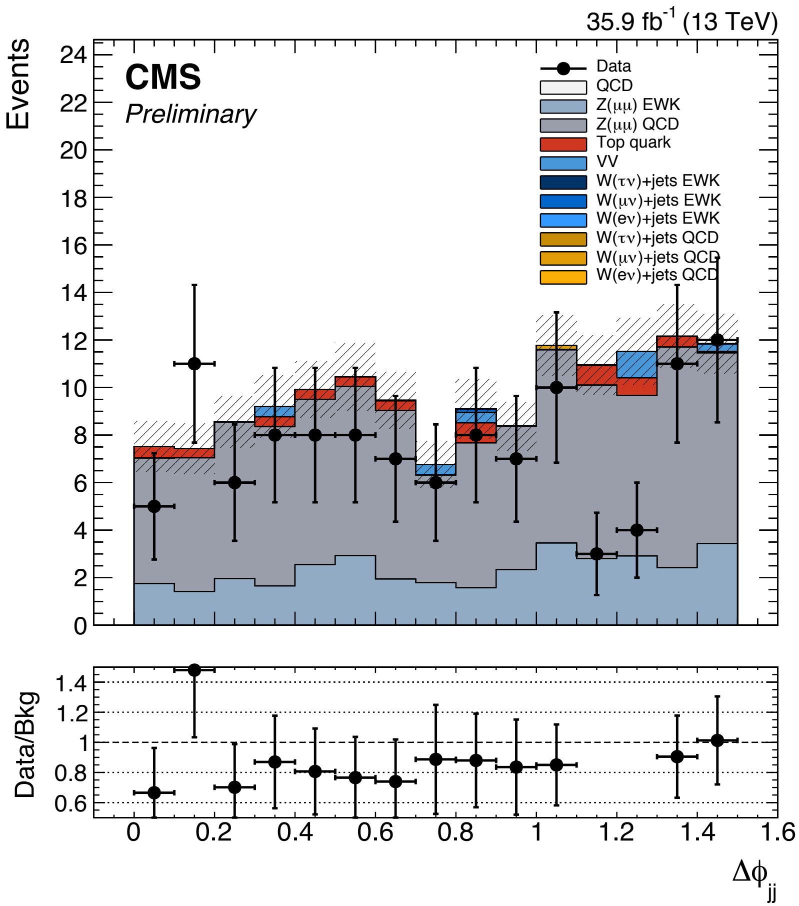

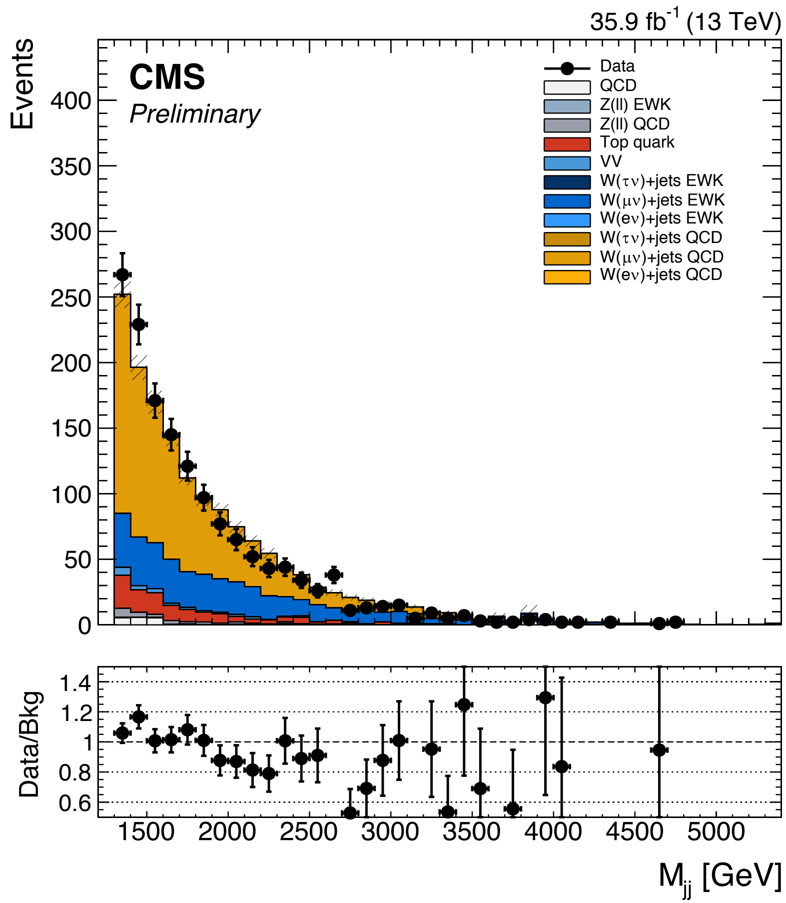

Electron CRs

- Events selected using $p_T^{single\text{-}electron}{}_{trig}$ with threshold of 27 GeV and 105 GeV, and imposing ISO requirements due to trigger inefficiency for Z-p_T > 600 GeV.
  - 2 oppositely charged e with p_T > 10 GeV:
    - at least one with p_T > 40 GeV that passes tighter ID;
    - 60 < m_{ee} < 120 GeV.
  - 1 e with p_T > 40 GeV, passing both tight ID and ISO requirements.
  - m_T < 160 GeV for the electron-MET system, and p_T^{miss} > 60 GeV to further reduce QCD multijet contamination.

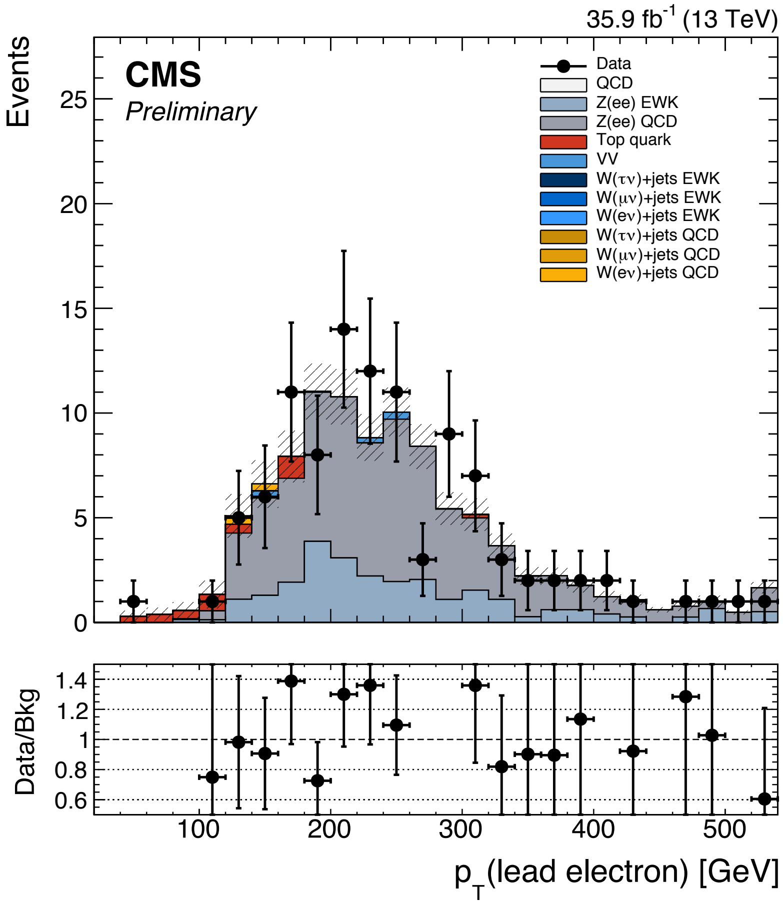

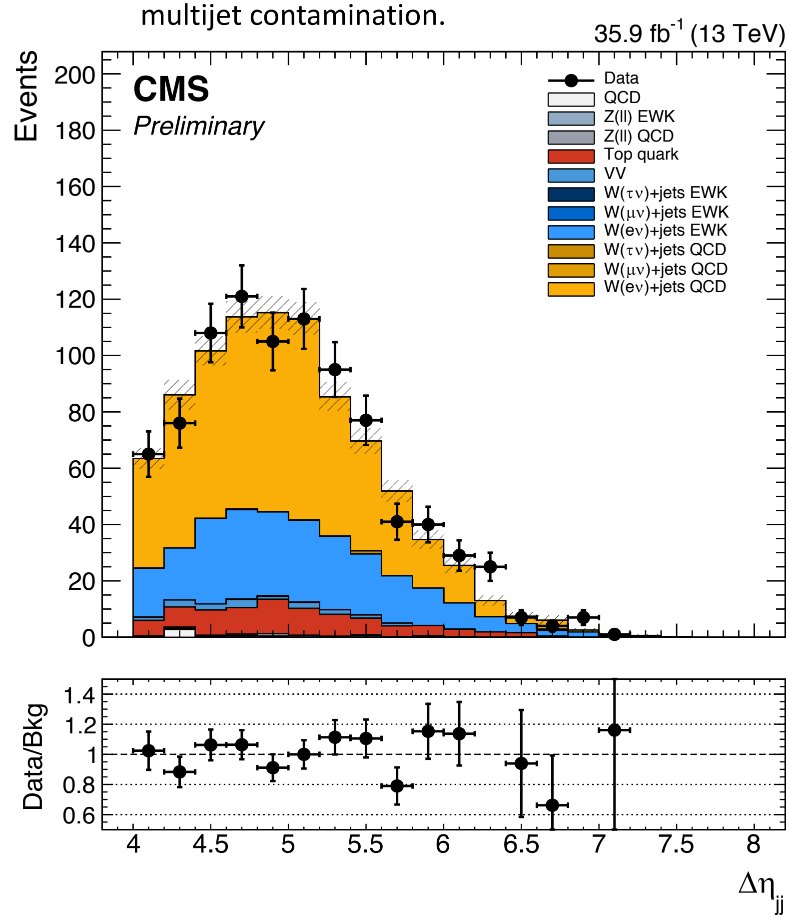

V+jets Background Estimation

- Z(νν) and W+jets backgrounds in the SR are measured primarily via leptonic CRs.
- Connection between SR and CRs performed via transfer factors (TFs) from MC.
- Background estimates in SR derived via V+jets yields in CRs for each m_{jj} bin.
- TFs account for differences in BR and acceptance (i.e. DY->ℓℓ vs. Z(νν)).
- TFs corrected for experimental effects via efficiencies/scale-factors measured in data.

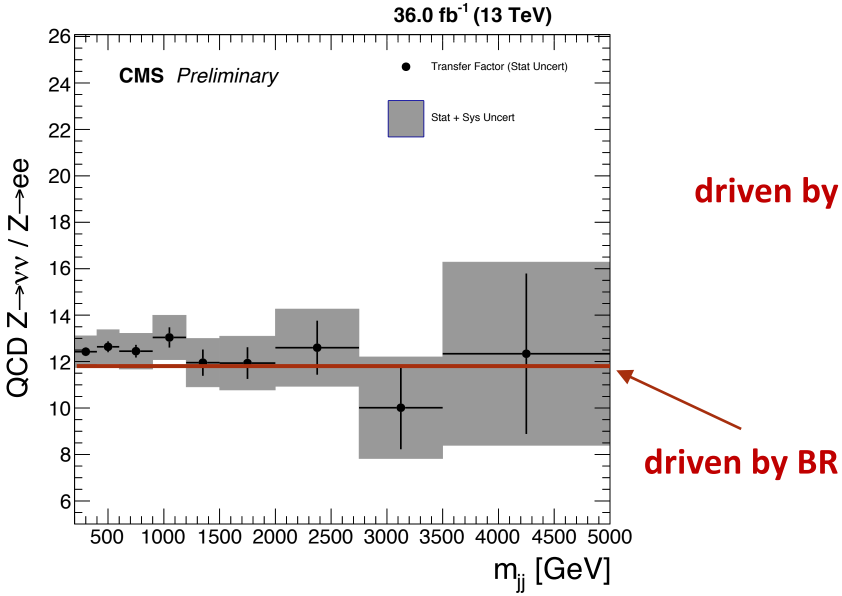

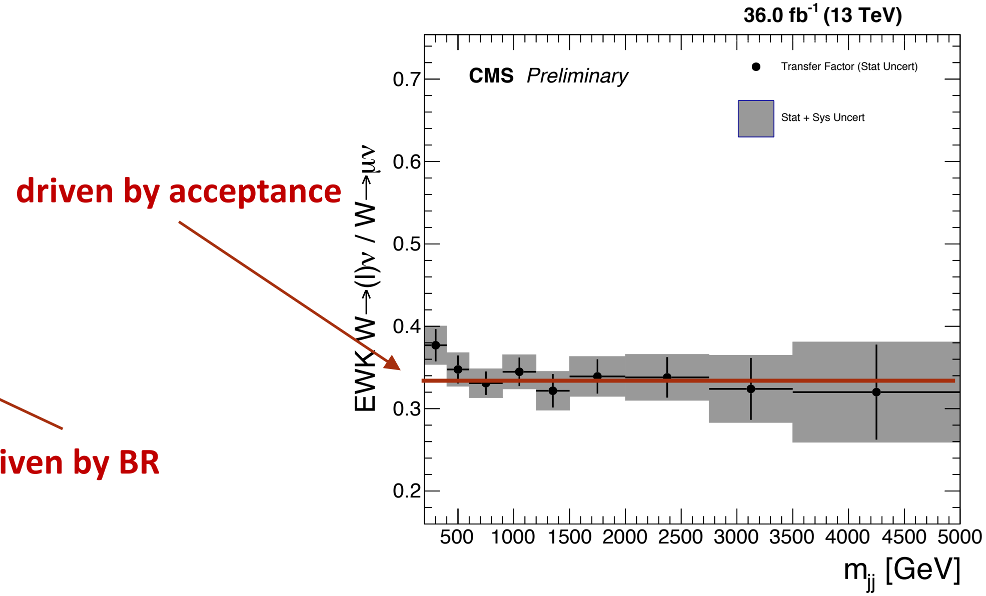

Cut-and-Count Signal Region

Process	Signal Region	Dimuon CR	Dielectron CR	Single-Muon CR	Single-Electron CR
$Z(\nu\nu)$ (QCD)	799 ± 72	-	-	-	-
$Z(\nu\nu)$ (EW)	275 ± 34	-	-	-	-
$Z(\ell\ell)$ (QCD)	-	90.1 ± 7.9	64.7 ± 5.8	26.8 ± 1.2	4.9 ± 0.2
$Z(\ell\ell)$ (EW)	-	32.7 ± 4.3	25.0 ± 3.4	5.9 ± 0.3	2.4 ± 0.2
$W(\ell\nu)$ (QCD)	497 ± 33	0.2 ± 0.2	0.8 ± 0.6	891 ± 31	533 ± 21
$W(\ell\nu)$ (EW)	145 ± 11	0.1 ± 0.1	-	416 ± 16	260 ± 11
Top-quark	43.7 ± 9.8	5.3 ± 1.6	3.7 ± 1.1	126 ± 22	83.1 ± 15.4
Dibosons	19.9 ± 6.1	2.6 ± 1.3	0.9 ± 0.5	23.5 ± 4.9	16.1 ± 4.1
Others	3.3 ± 2.6	-	-	25.6 ± 20.7	2.9 ± 2.9
Total Bkg.	1784 ± 97	131 ± 8	95.2 ± 5.9	1515 ± 34	902 ± 24
Data	2053	114	104	1512	914
Signal $m_H = 125$ GeV	851 ± 148	-	-	-	-

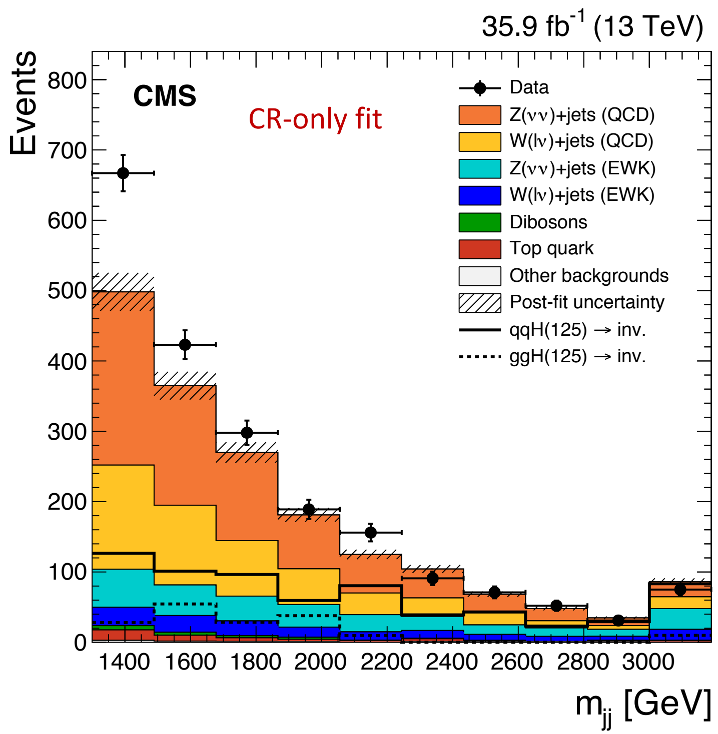

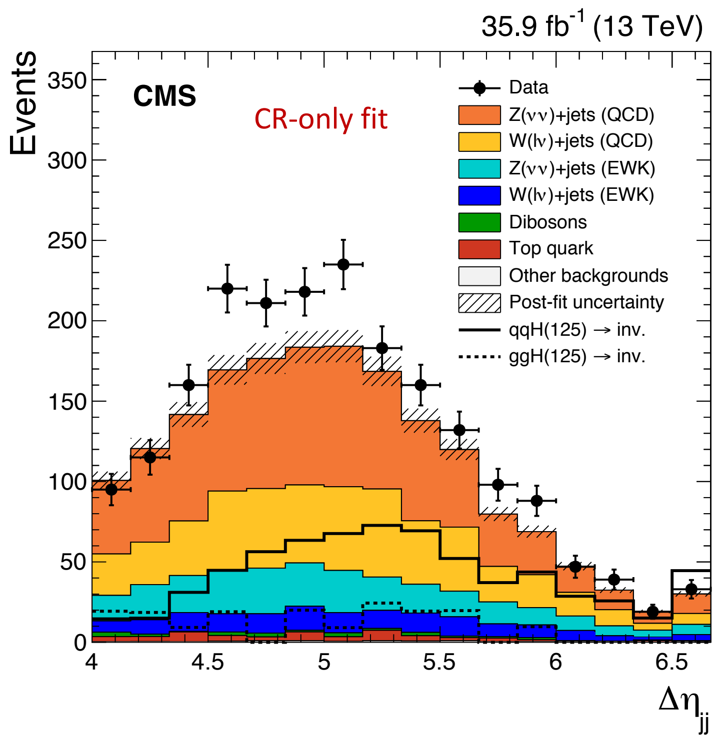

Upper Limits on $\mathcal{B}$(H(inv.))

- The observed and expected 95% confidence level upper limits on $\mathcal{B}$(H(inv.)) assuming SM production rate are:

Analysis	Observed limit	Expected limit	±1 s.d.	±2 s.d.	Signal composition
Shape	0.28	0.21	[0.15–0.29]	[0.11–0.39]	52% qqH, 48% ggH
Cut-and-count	0.53	0.27	[0.20–0.38]	[0.15–0.51]	81% qqH, 19% ggH

- Upper limits vs. m_H for BSM Higgs boson benchmark.

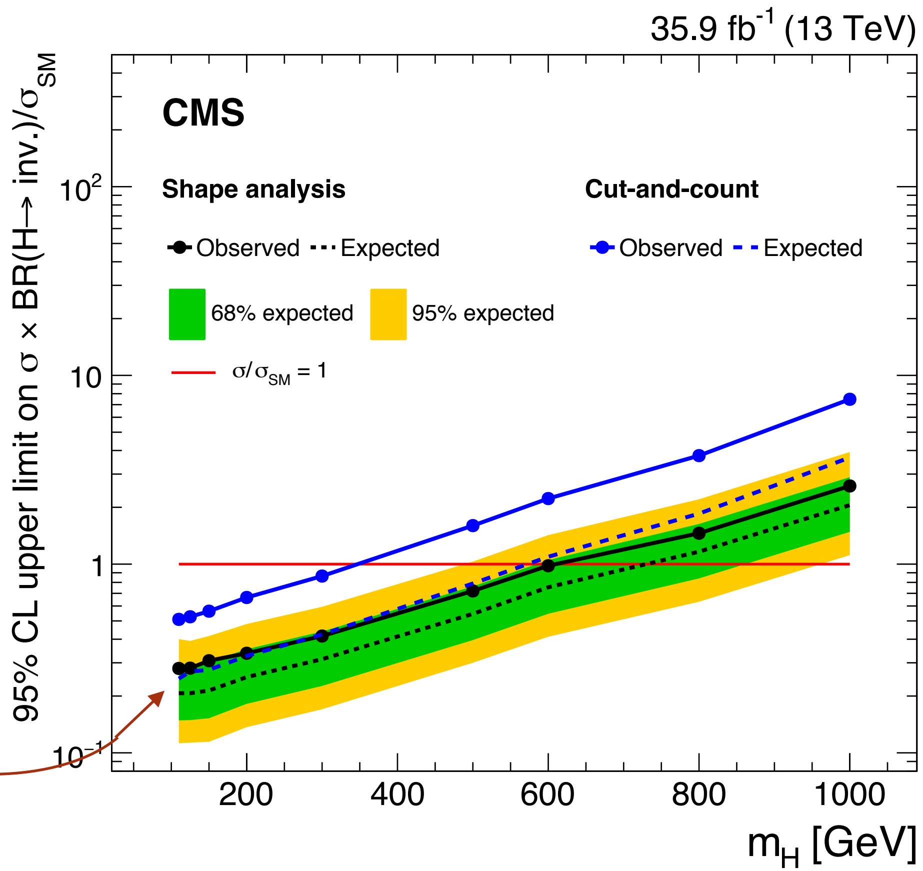

Combination of H(inv.) Searches

Analysis	Final state	Signal composition	Observed limit	Expected limit
qqH-tagged	VBF-jets + p_T^{miss}	52% qqH, 48% ggH	0.28	0.21
VH-tagged	$Z(\ell\ell) + p_T^{miss}$ [11]	79% qqZH, 21% ggZH	0.40	0.42
	$V(qq') + p_T^{miss}$ [12]	40% ggH, 3% qqH, 35% WH, 22% ZH	0.50	0.48
ggH-tagged	jets + p_T^{miss} [12]	80% ggH, 9% qqH, 6% WH, 5% ZH	0.64	0.58

- [11] **CMS EXO-16-052**
- [12] **CMS EXO-16-048**
- The overlap between the various searches has been removed.

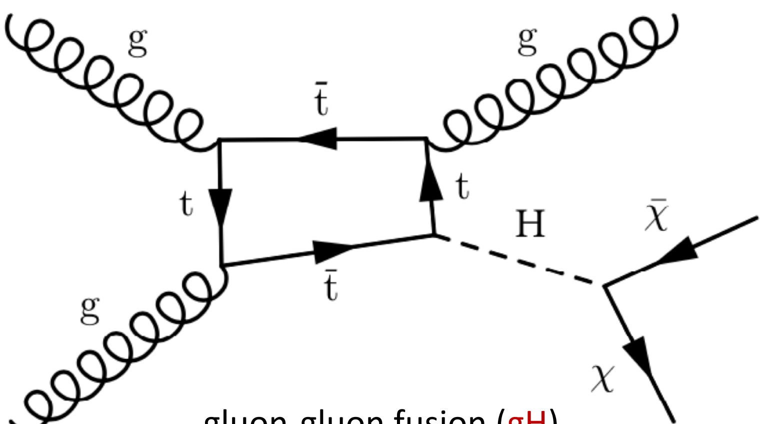

gluon-gluon fusion (gH)

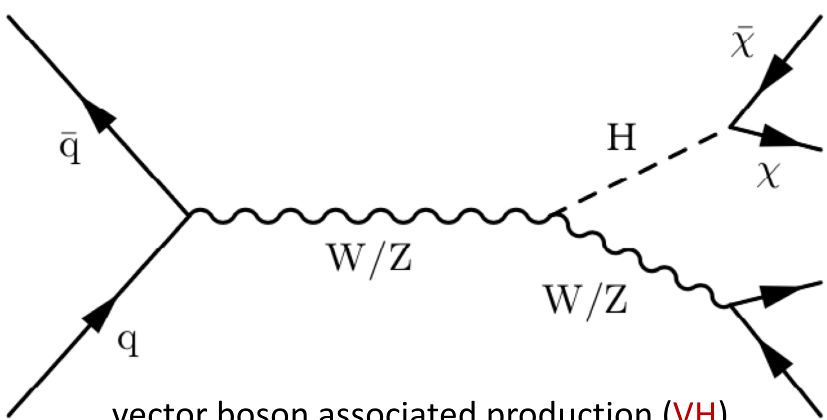

vector boson associated production (VH)

Combination of H(inv.) Searches

- The observed (expected) 95% confidence level upper limits on $\mathcal{B}$(H(inv.)) assuming SM production rate is: **0.24 (0.18)**.

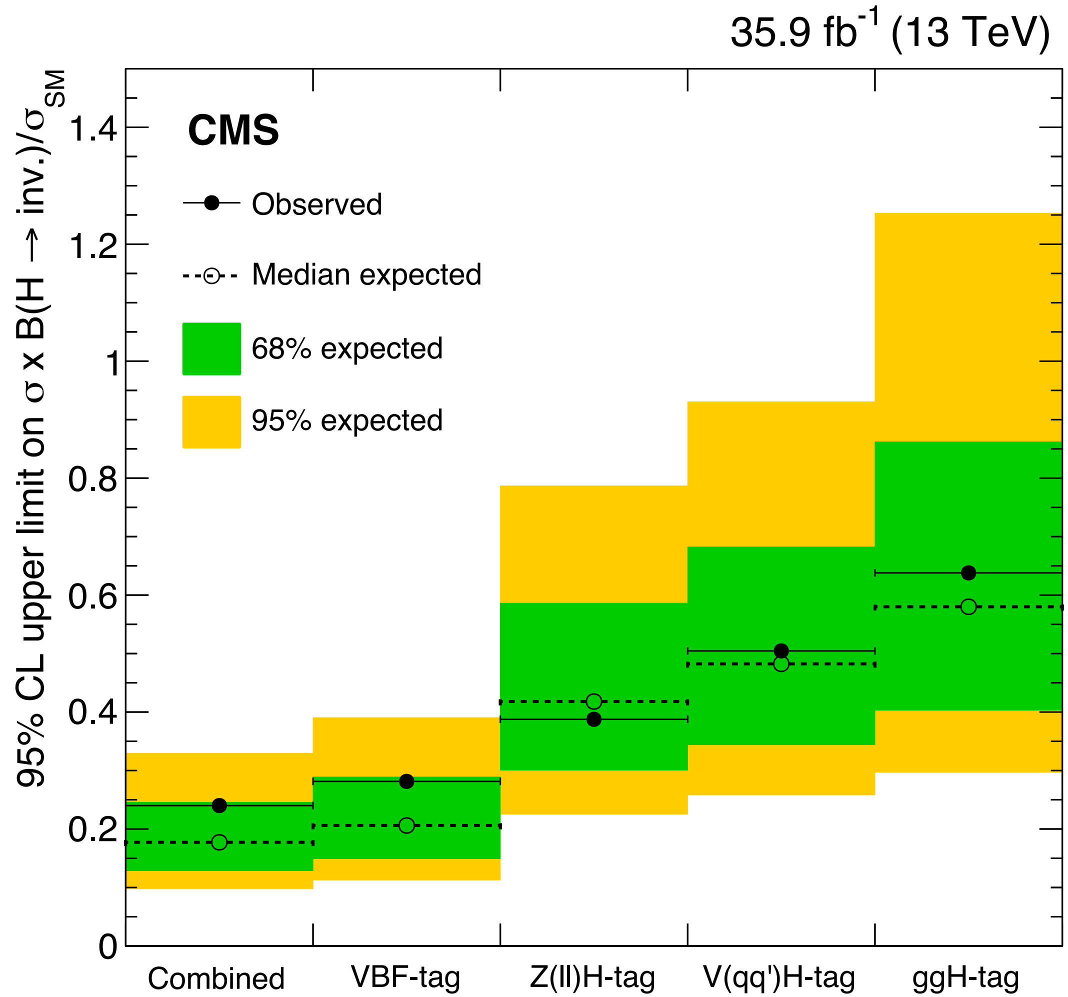

DM Interpretation

- $\mathcal{B}$(H(inv.)) translated into DM-nucleon spin-independent cross-section limits as a function of DM mass (90% CL to compare to direct detection experiments).
- Use Higgs-Portal models [9] assuming **scalar**/**fermion** DM candidate.
- LHC limits complementary to direct detection experiments.

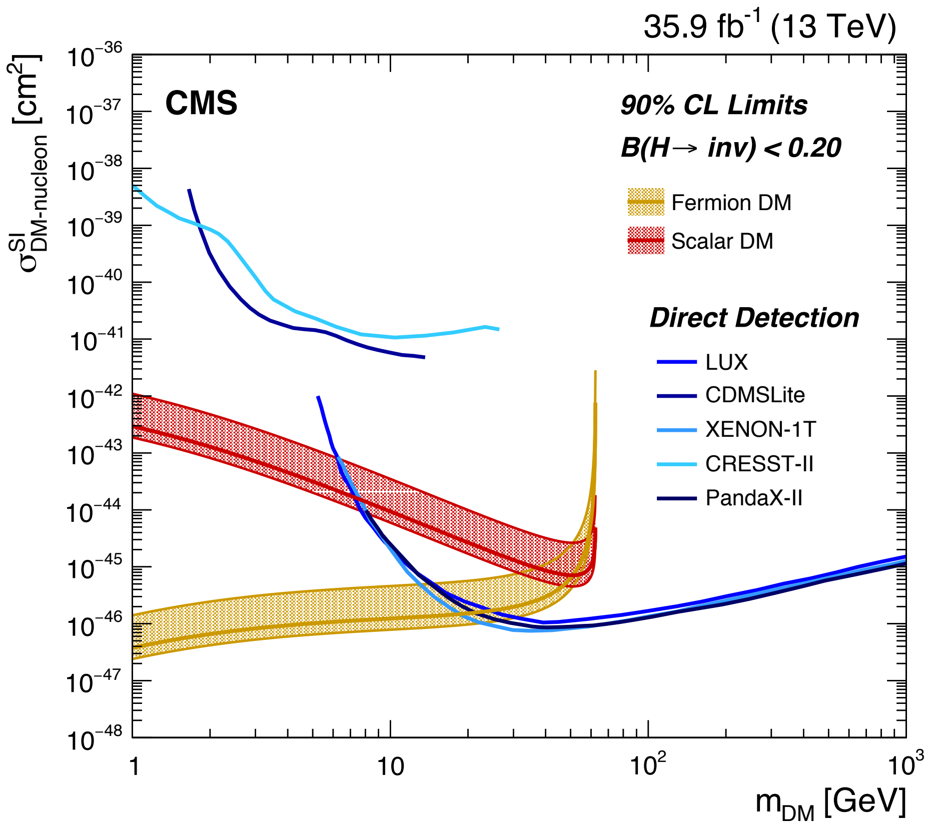

Conclusions

- Direct search for Higgs boson decays to invisible final states has been carried out in the VBF production channel.

HIG-17-023	Observed (Expected) Upper Limit @ 95% CL on $\mathcal{B}$(H(inv.))
Cut-and-count	**0.53 (0.27)**
Shape	**0.28 (0.21)**
Combination	**0.24 (0.18)**

Reference	Observed (Expected) Upper Limit @ 95% CL on $\mathcal{B}$(H(inv.))
HIG-16-016 VBF-only (C&C Run1+Run2)	0.44 (0.31)
CMS JHEP 02 (2017) 135 arXiv:1610.09218	0.24 (0.23)
ATLAS JHEP 11 (2015) 206 arXiv:1509.00672	0.25 (0.27)

- A DM interpretation has been provided, translating $\mathcal{B}$(H(inv.)) into DM-nucleon spin-independent cross-section limits as a function of DM mass.

Backup Slides

Dark Matter

- The dark matter is supposed to be a thermal relic of the early Universe.
- The comparison between direct and indirect detection is model dependent.
- A theoretical guidance is needed (LHC DM forum).

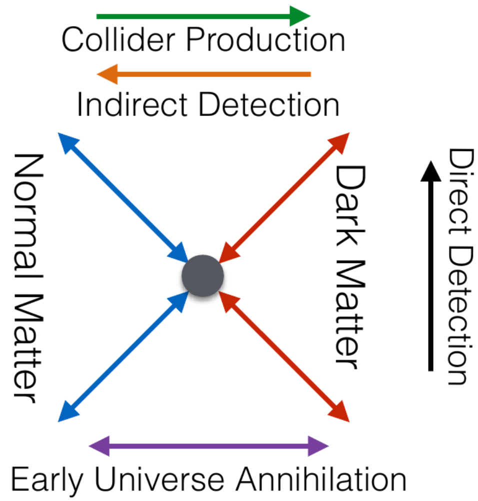

arXiv:1603.04156

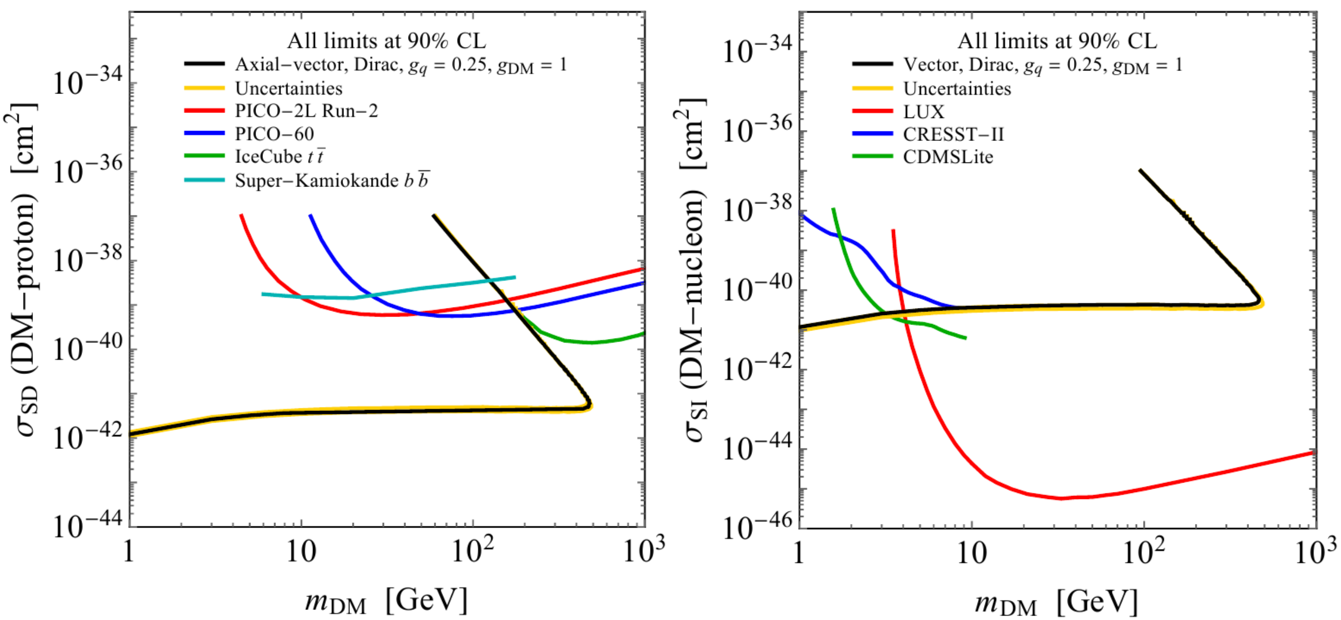

The CMS Experiment

- All the CMS sub-detectors are vital for MET-searches.

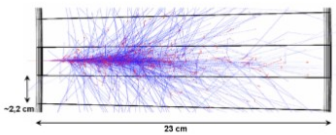

EM Calorimeter
Lead tungstate (PbWO4) crystals
61 200 (EB) / 7 324 (EE)

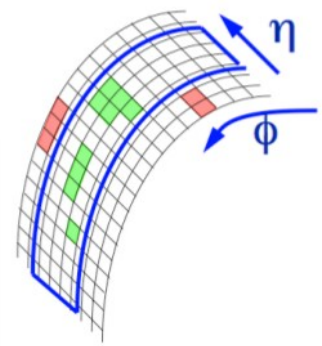

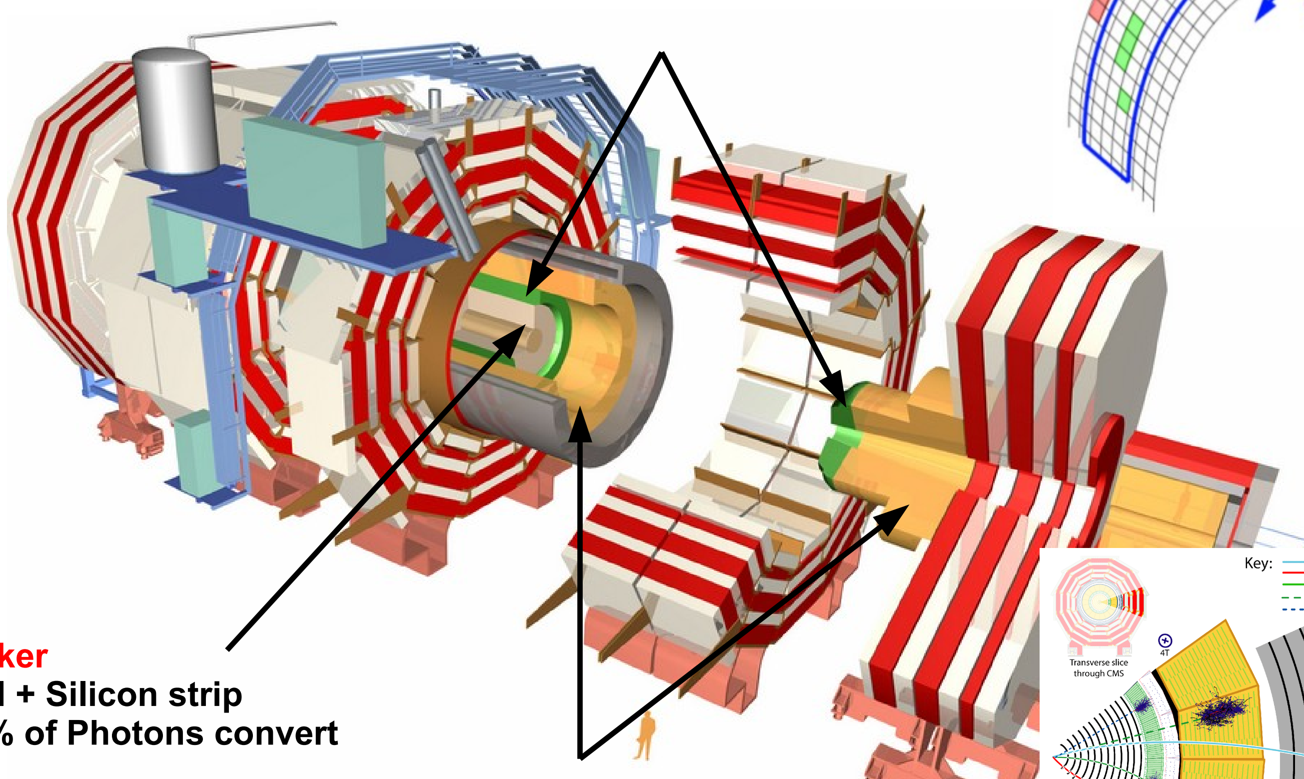

Tracker
Pixel + Silicon strip
~50% of Photons convert

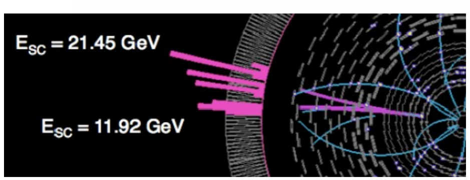

Hadron Calorimeter
Scintillating Brass
Exploit jets from VBF production

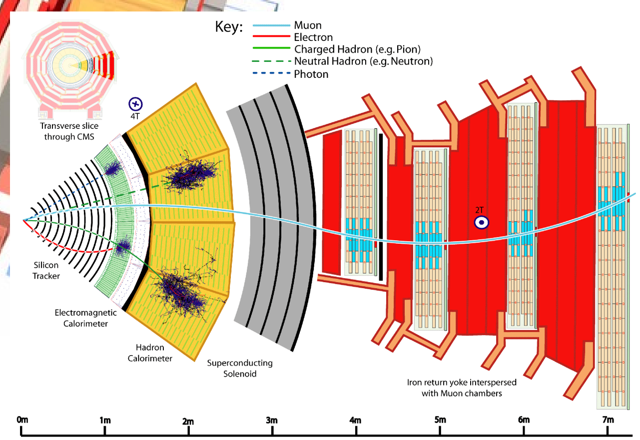

Signal Kinematics

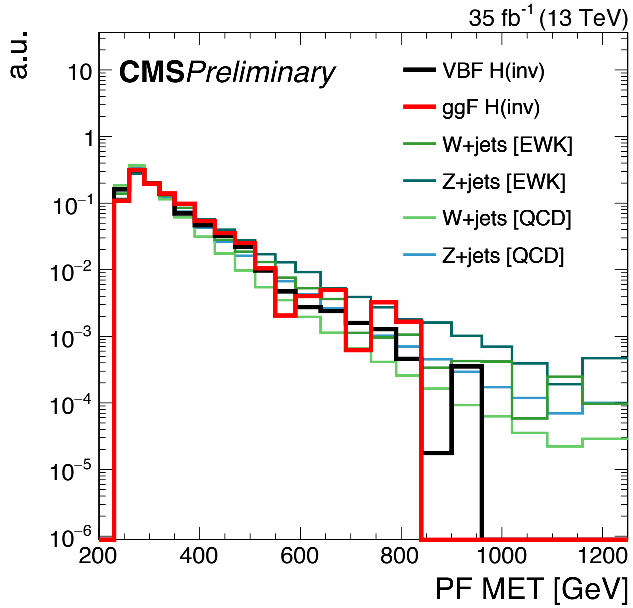

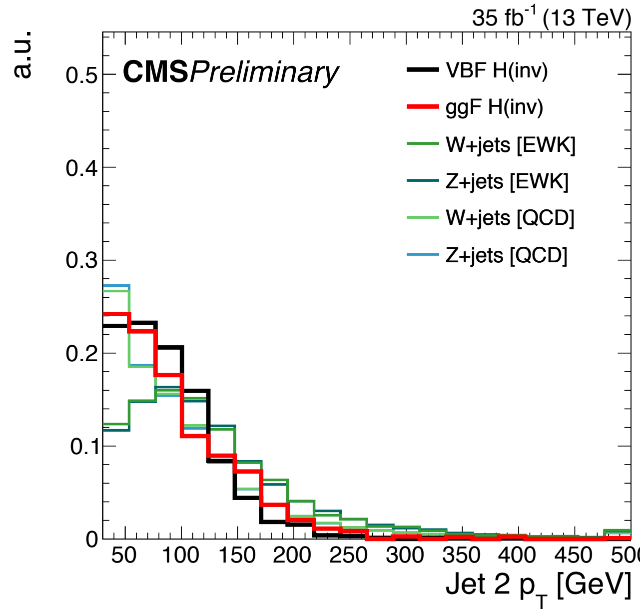

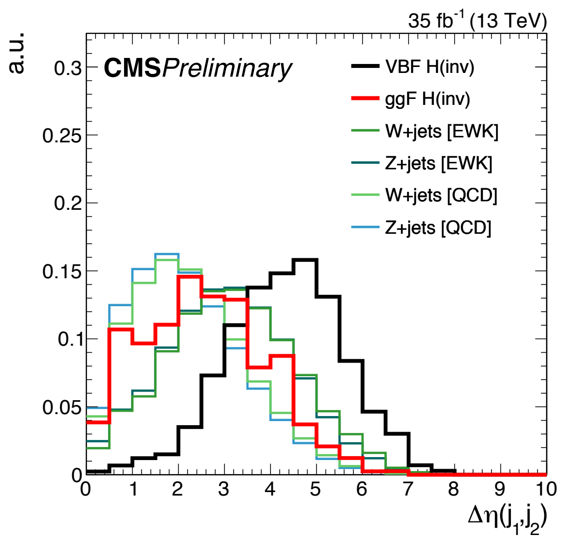

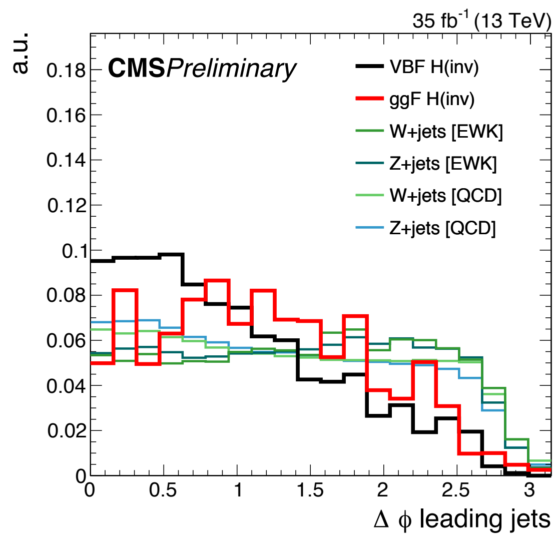

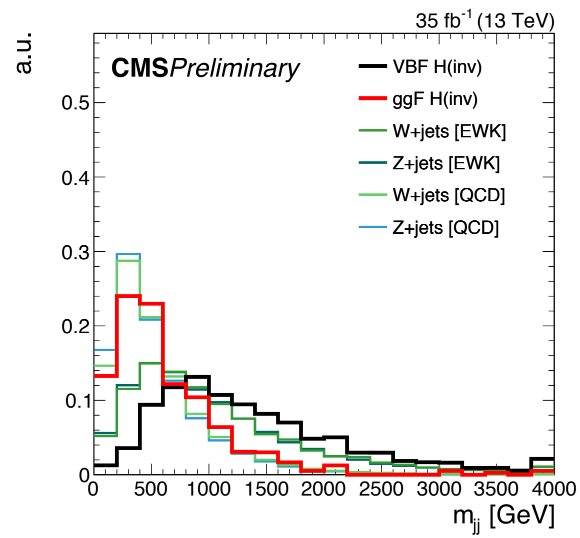

Simulation and Object Corrections

- qqH and ggH signals: Powheg2.0 at NLO in QCD, normalised to the $\sigma_H^{inclusive}$ from YR4 [arXiv:1610.07922].

- Z/γ*(ℓℓ)+jets
- Z(νν)+jets
- W(ℓν)+jets
- EWK V+jets
- QCD multijet

} LO using MadGraph5_aMC@NLO

- ttbar
- single top quark
- WW

} NLO QCD using Powheg

- WZ
- ZZ

} LO with Pythia8.205

- Following POG recommendations, e.g. lepton ID and reco efficiencies, hadronic-tau ID, b-tagging efficiencies, jet energy corrections…

NLO Corrections

- (LO QCD, EWK)-Z+jets and (QCD, EWK)-W+jets are corrected with NLO-QCD k-factors as a function of boson p_T and m_{jj}.

- QCD k-factors derived in VBF phase space.

- Large NLO-QCD corrections for QCD-V+jets as shown in the plot.

- Important impact on the analysis:

    - e.g. change the Z/W ratio.

- Smaller NLO-QCD corrections for EWK-V+jets (as expected), ranging between 3-10%

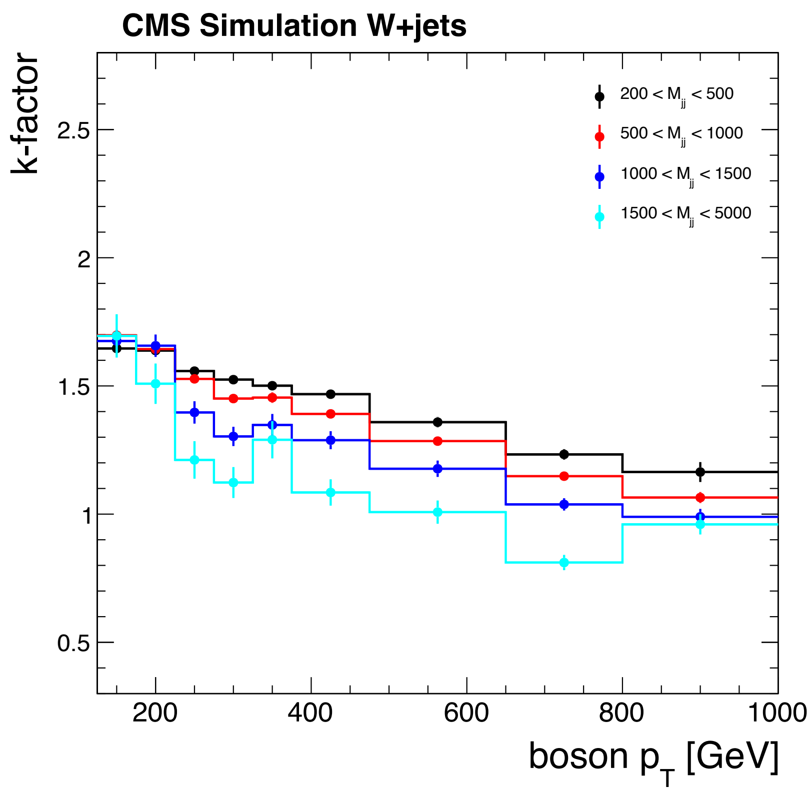

- The QCD-Z+jets and QCD-W+jets are also corrected with p_T-dependent NLO EWK corrections (from theoretical calculation).

Trigger Selection

- At L1, p_T^{miss}-based triggers ([60,90] GeV) are used to select signal region (SR) events.
- At HLT, triggers with thresholds of 110 or 120 GeV are used, applied to $p_T^{miss}{}_{trig}$ and $H_T^{miss}{}_{trig}$ without including muons (same triggers for muon control regions (CR)).
- Since the L1 decision is blind to hadronic activity in HF, leading OR trailing jet with $|\eta| < 3$.
- Trigger efficiency parametrised vs offline H_T^{miss}, stable as a function of jets kinematics (B = jet $|\eta| < 3$, F = jet $|\eta| > 3$ i.e. HF).

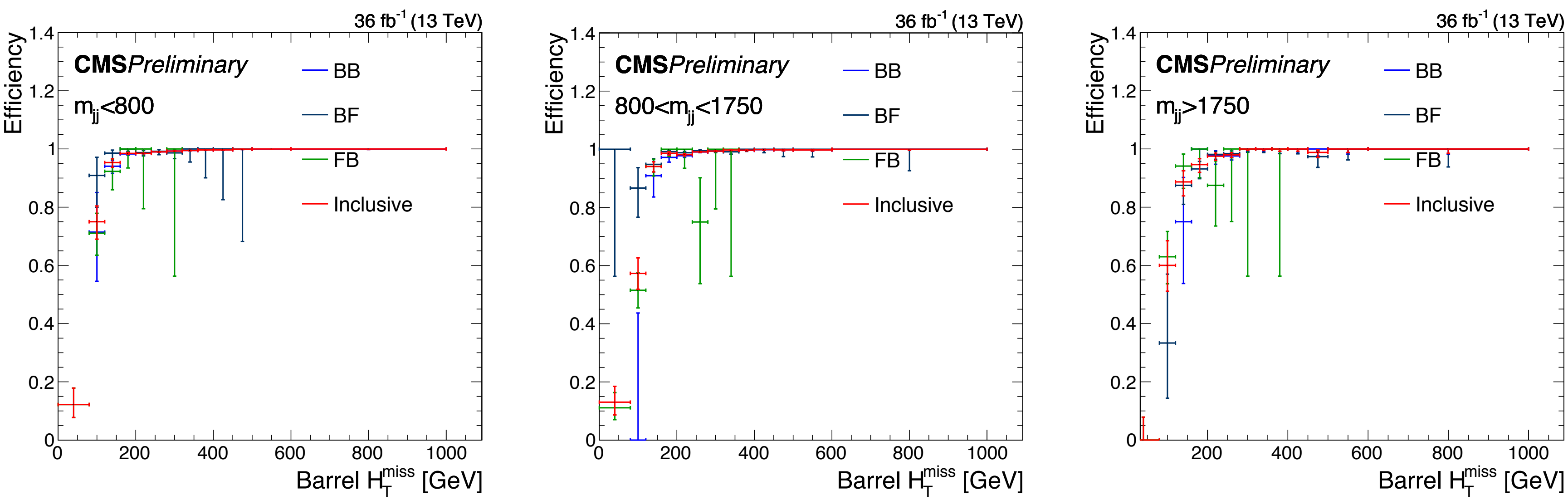

V+jets Background Estimation

- Z/W constraint used to improve the precision on Z(vv) estimate, exploiting the larger statistical power of the single-lepton CRs.
- Z/W ratio between CRs: important to cross-check the effect of higher order corrections and if data-to-MC differences are covered by the uncertainties.
- Z/W ratio affected mainly by theoretical systematics.

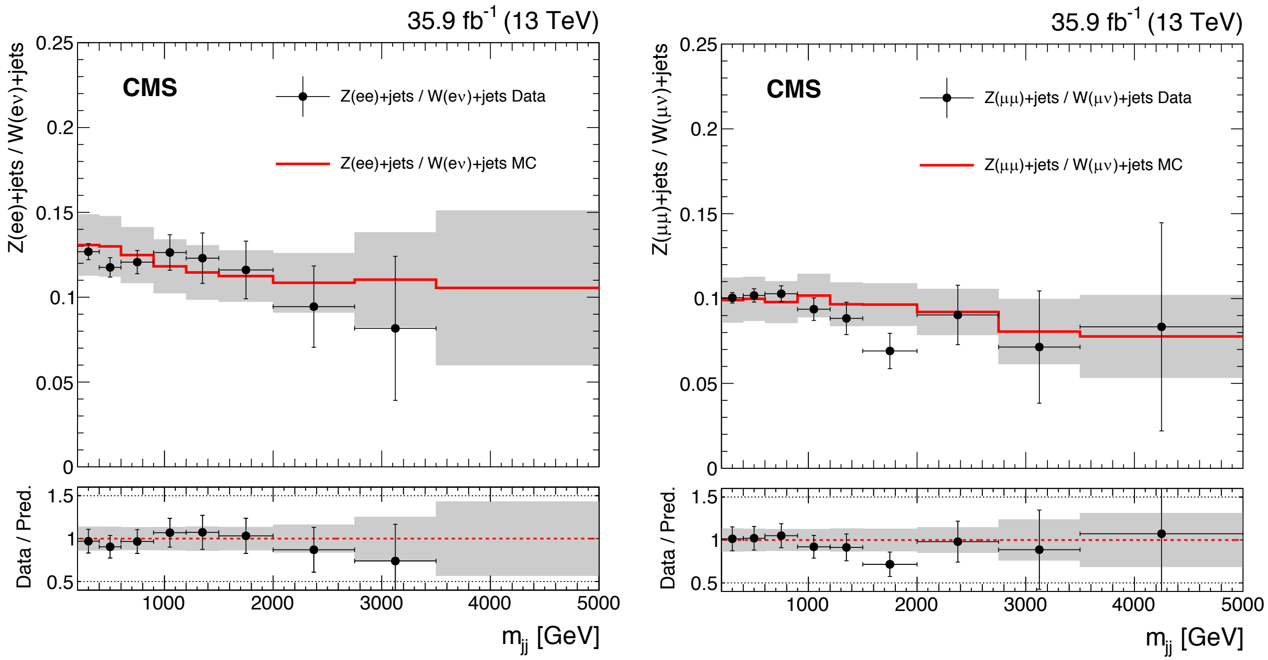

- Gray bands include both the pre-fit systematic uncertainties and the statistical uncertainty in the simulation.

QCD Estimation

- A QCD multijet enriched CR with inverted Δϕ and p_T^{miss} SR selections is used to estimate this background from data.
- The contamination from V+jets backgrounds in the low-Δϕ region is estimated from simulation and subtracted (20% unc.) from the event yield measured.
- The QCD multijet MC statistical uncertainty varies between 40-100% as a function of m_{jj}.

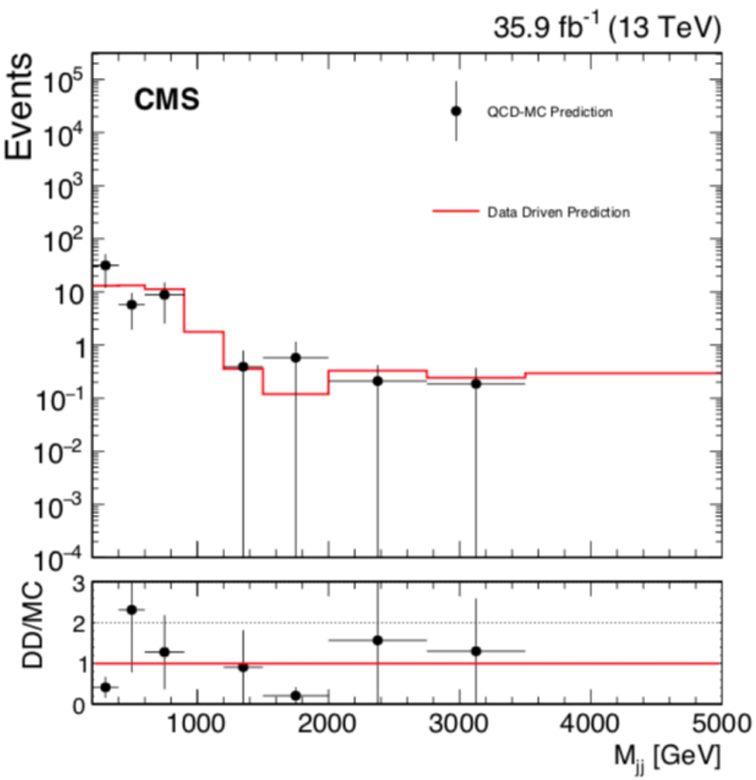

Systematic Uncertainties

- Systematic uncertainties are modelled as constrained nuisance parameters.
- Z(νν)+jets and W(lν)+jets backgrounds uncertainties enter in the likelihood as variations of the TFs.

Source of uncertainty	Ratios	Uncertainty vs m_{jj}	Impact on $\sigma\mathcal{B}(H \to inv)/\sigma_{SM}$
	Theoretical uncertainties		
Renorm. scale V+jets (EW)	$Z(\nu\nu)/W(\ell\nu)$ (EW)	9–12%	48%
Renorm. scale V+jets (QCD)	$Z(\nu\nu)/W(\ell\nu)$ (QCD)	9–12%	23%
Fact. scale V+jets (EW)	$Z(\nu\nu)/W(\ell\nu)$ (EW)	2–7%	4%
Fact. scale V+jets (QCD)	$Z(\nu\nu)/W(\ell\nu)$ (QCD)	2–7%	2%
NLO EW corr.	$Z(\nu\nu)/W(\ell\nu)$ (QCD)	1–2%	$< 1\%$
PDF V+jets (QCD)	$Z(\nu\nu)/W(\ell\nu)$ (QCD)	0.5–1%	$< 1\%$
PDF V+jets (EW)	$Z(\nu\nu)/W(\ell\nu)$ (EW)	0.5–1%	$< 1\%$
	Experimental uncertainties		
p_T^{miss} trigger	All ratios	$\approx 2\%$	18%
Muon id. eff.	$W(\mu\nu)/W(\ell\nu)$, $Z(\mu\mu)/Z(\nu\nu)$	$\approx 1\%$ (per leg)	8%
Muon reco. eff.	$W(\mu\nu)/W(\ell\nu)$, $Z(\mu\mu)/Z(\nu\nu)$	$\approx 1\%$ (per leg)	8%
Ele. id. eff.	$W(e\nu)/W(\ell\nu)$, $Z(ee)/Z(\nu\nu)$	$\approx 1.5\%$ (per leg)	4%
Ele. reco. eff.	$W(e\nu)/W(\ell\nu)$, $Z(ee)/Z(\nu\nu)$	$\approx 1\%$ (per leg)	3%
τ veto	$W(CRs)/W(\ell\nu)$, $Z(\nu\nu)/W(\ell\nu)$	≈ 3.5 (3)% for EW (QCD)	13%
Muon veto	$W(CRs)/W(\ell\nu)$, $Z(\nu\nu)/W(\ell\nu)$	≈ 2.5 (2)% for EW (QCD)	7%
Ele. veto	$W(CRs)/W(\ell\nu)$, $Z(\nu\nu)/W(\ell\nu)$	≈ 1.5 (1)% for EW (QCD)	5%
Jet energy scale	$Z(CRs)/Z(\nu\nu)$, $W(CRs)/W(\ell\nu)$	≈ 1 (2)% for Z/Z (W/W)	2%
Ele. trigger	$W(e\nu)/W(\ell\nu)$, $Z(ee)/Z(\nu\nu)$	$\approx 1\%$	$< 1\%$

- Systematic uncertainties on minor backgrounds detailed in backup.
- Before the fit, the total uncertainty in the background estimation in SR is [4.5,6]% as a function of m_{jj}.

Additional Uncertainties

Source	Uncertainty
QCD multijet	30% + conservative 50% from Δϕ method validation
Diboson normalisation	15%
Top quark normalisation	10%
Modelling of the Top quark p_T distribution in simulation	10%
b-jet veto for Top quark	3%
b-jet veto for other simulated processes	≈1%
JES	8-15%
Integrated luminosity	2.5%

Event Selection

- Both for *cut-and-count* and *shape*, selection and binning optimised wrt best exclusion limit on $\mathcal{B}$(H(inv.)).
- Optimisation studies performed on $\Delta\eta_{jj}$, $\Delta\phi_{jj}$, and m_{jj}.
- Among the various variables, m_{jj} most sensitive.

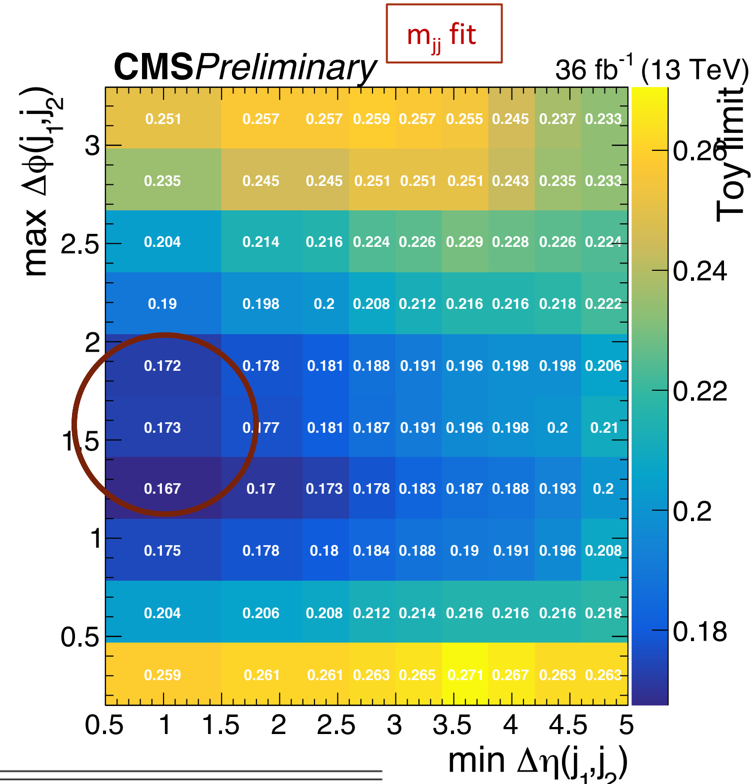

Observable	Shape analysis	Cut-and-count analysis	Target background
Leading (trailing) jet	$p_T > 80$ (40) GeV, $\lvert\eta\rvert < 4.7$		All
p_T^{miss}	> 250 GeV		QCD multijet, $t\bar{t}$, W + jets
$\Delta\phi(p_T^{miss}, p_T^{jet})$	> 0.5		QCD multijet
$\lvert\Delta\phi_{jj}\rvert$	< 1.5 radians		$Z(\nu\bar{\nu})$+jets, $W(l\nu)$+jets
$\eta_{j1} \cdot \eta_{j2}$	< 0		$Z(\nu\bar{\nu})$+jets, $W(l\nu)$+jets
$\lvert\Delta\eta_{jj}\rvert$	> 1	> 4	$Z(\nu\bar{\nu})$+jets, $W(l\nu)$+jets
$\lvert m_{jj}\rvert$	> 200 GeV	> 1300 GeV	$Z(\nu\bar{\nu})$+jets, $W(l\nu)$+jets
Muons and electrons	$N_{\mu,e} = 0$ with $p_T > 10$ GeV, $\lvert\eta\rvert < 2.4$ (2.5)		W + jets, $Z(ll)$+jets
τ leptons	$N_{\tau_h} = 0$ with $p_T > 18$ GeV, $\lvert\eta\rvert < 2.3$		W + jets, $Z(ll)$+jets
Photons	$N_\gamma = 0$ with $p_T > 15$ GeV, $\lvert\eta\rvert < 2.5$		γ+jets, $V\gamma$
B-jets	$N_{jet} = 0$ with $p_T > 20$ GeV, CSVv2 > 0.8484		$t\bar{t}$, single top

Control Regions

- The V+jets represent the largest backgrounds in this search (≈95%).
- The V+jets backgrounds are determined through a simultaneous maximum-likelihood fit across 4 CRs and SR.
- p_T^{miss} calculated excluding the p_T of the identified leptons (proxy for SR).
- Specific lepton(s) selections used to construct the CR.
- SR selection applied.
- Hadronic-τ, γ, and additional muon or electron rejected.

Muon CRs

- Events selected using the same SR $p_T^{miss}{}_{trig}$.

- 2 oppositely charged μ with $p_T > 10$ GeV:
  - at least one with $p_T > 20$ GeV that passes tighter ID;
  - $60 < m_{\mu\mu} < 120$ GeV.

- 1 μ with $p_T > 20$ GeV, passing both tight ID and ISO requirements.
- $m_T < 160$ GeV for the muon-MET system.

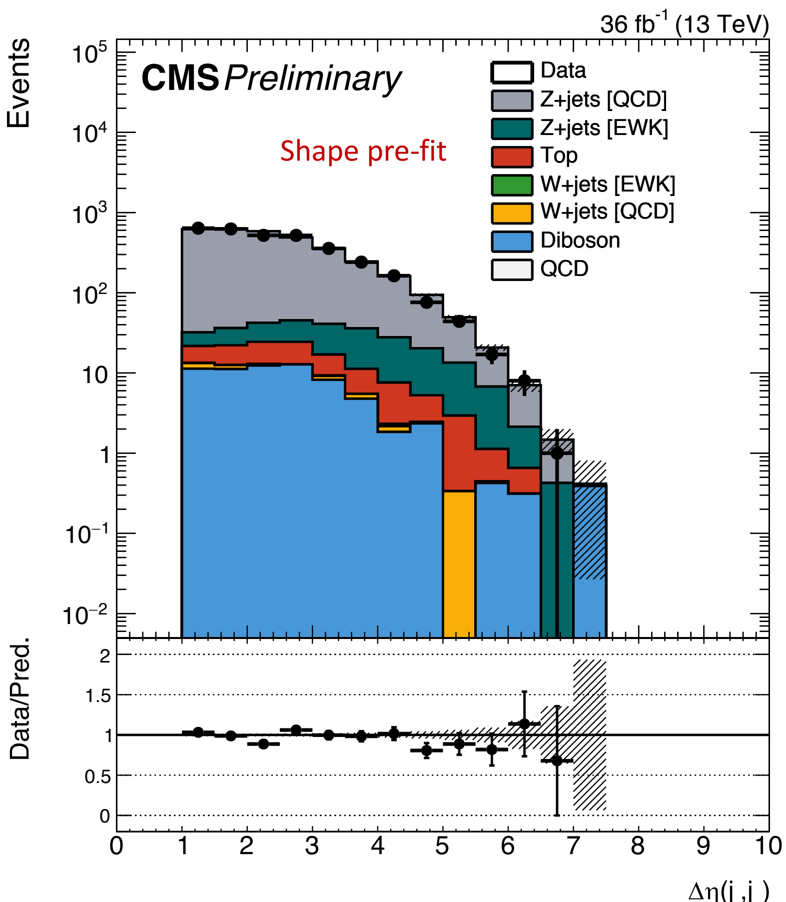

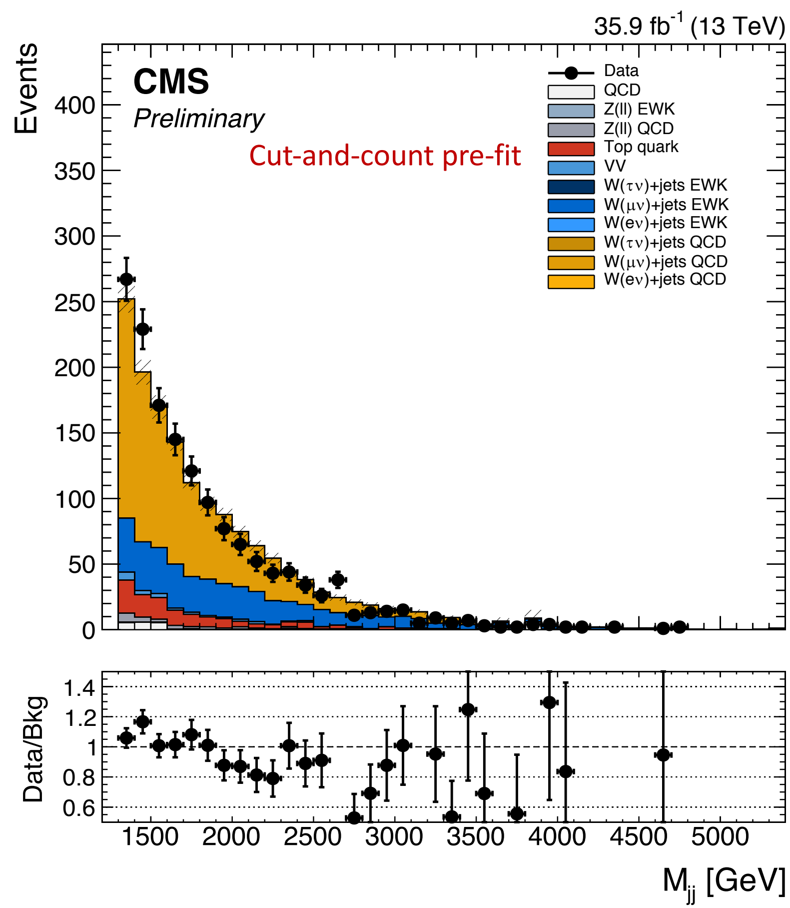

Electron CRs

- Events selected using $p_T^{single\text{-}electron}{}_{trig}$ with threshold of 27 GeV and 105 GeV, and imposing ISO requirements due to trigger inefficiency for Z-p_T > 600 GeV.

- 2 oppositely charged e with p_T > 10 GeV:
    - at least one with p_T > 40 GeV that passes tighter ID;
    - 60 < m_{ee} < 120 GeV.

- 1 e with p_T > 40 GeV, passing both tight ID and ISO requirements.
- m_T < 160 GeV for the electron-MET system, and p_T^{miss} > 60 GeV to further reduce QCD multijet contamination.

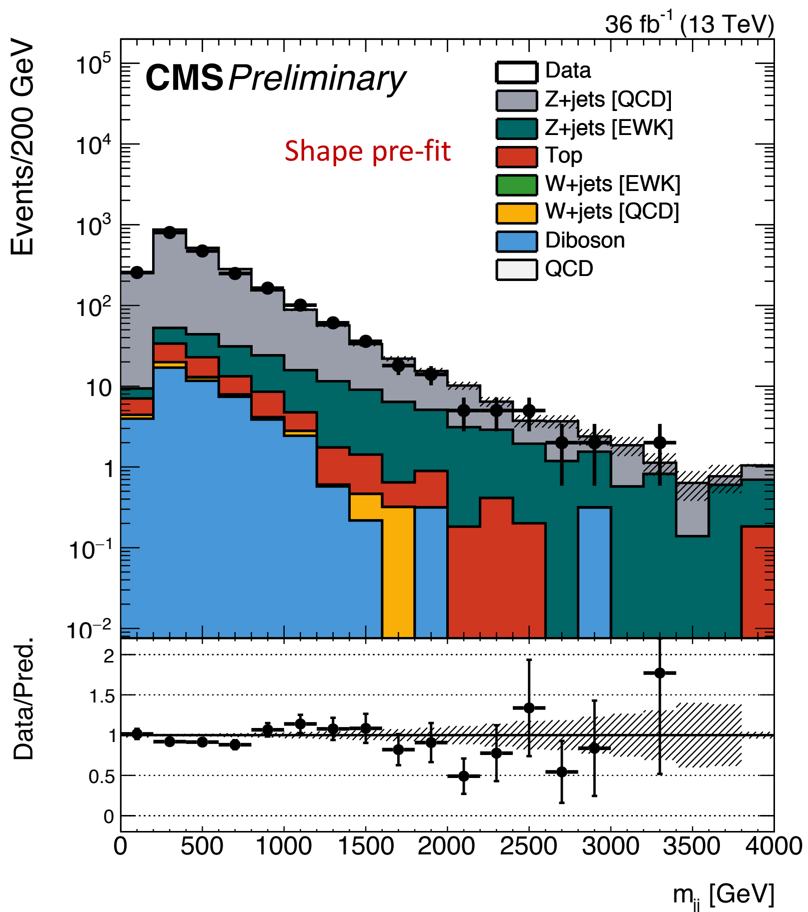

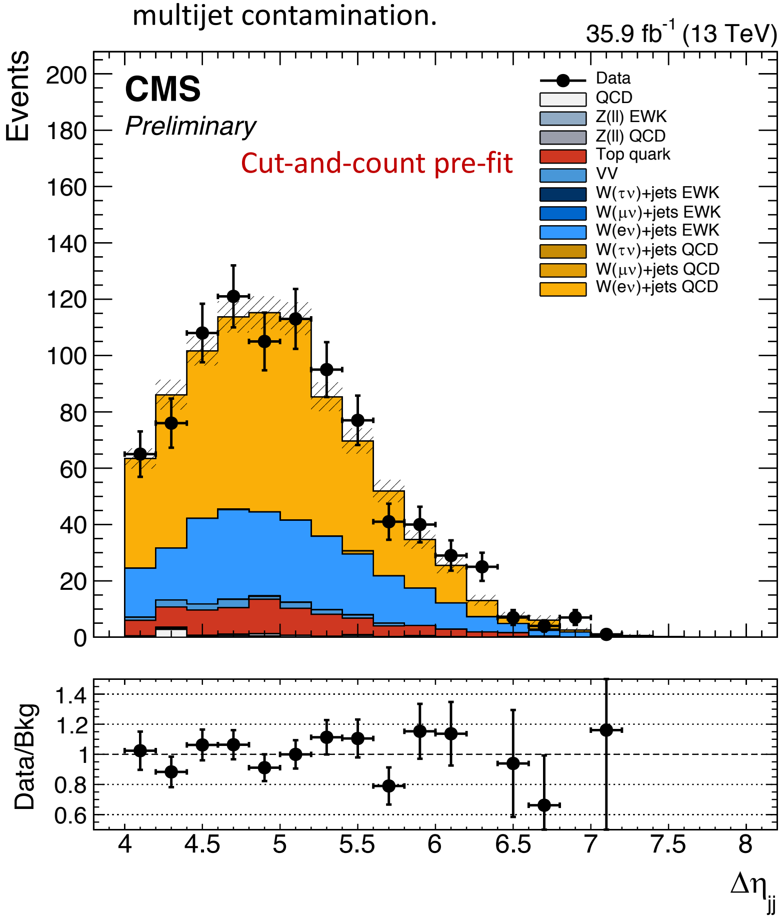

Shape Signal Region

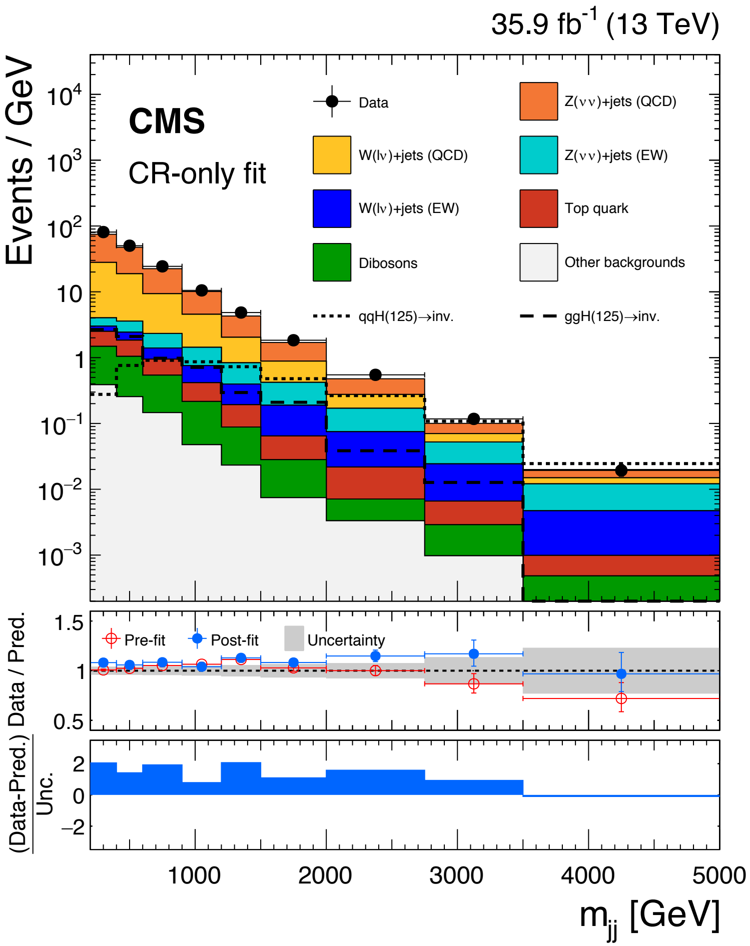

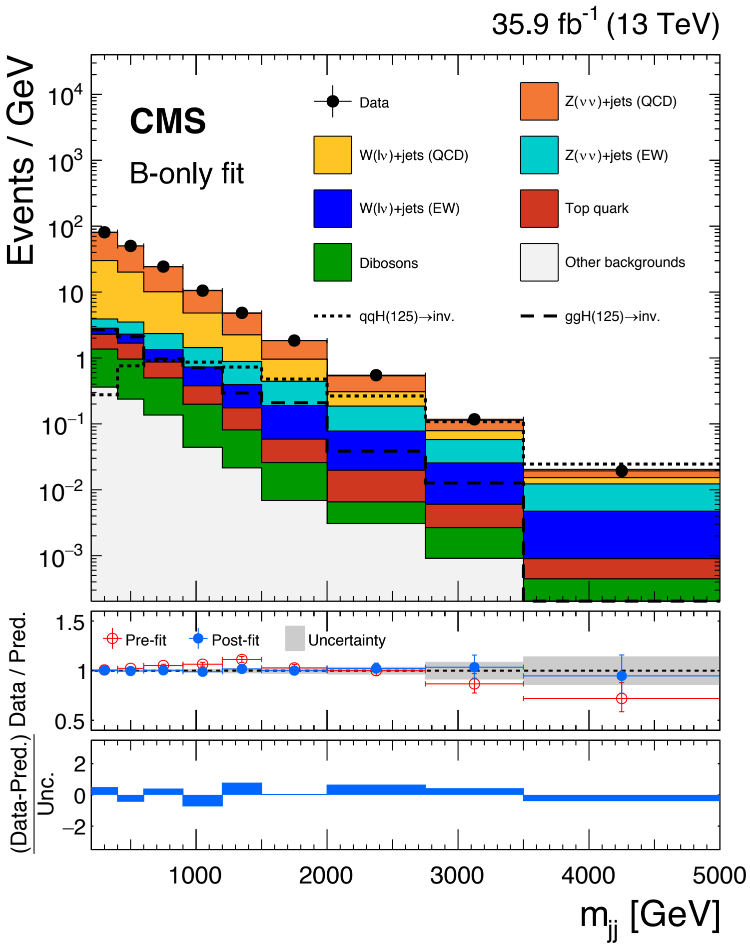

- Data in SR are excluded (left) and included (right) in the fit assuming the absence of any signal.

Shape Signal Region

	m_{jj} range in TeV								
Process	0.2–0.4	0.4–0.6	0.6–0.9	0.9–1.2	1.2–1.5	1.5–2.0	2.0–2.75	2.75–3.5	> 3.5
$Z(\nu\nu)$ (QCD)	9367 ± 394	5716 ± 256	3925 ± 184	1665 ± 84	675 ± 43	406 ± 26	151 ± 14	22.6 ± 3.6	7.5 ± 2.1
$Z(\nu\nu)$ (EW)	202 ± 8	230 ± 10	278 ± 13	203 ± 10	131 ± 8	115 ± 8	71.3 ± 6.6	20.9 ± 3.4	11.6 ± 3.1
$W(\ell\nu)$ (QCD)	4786 ± 252	3046 ± 165	2122 ± 125	936 ± 58	361 ± 29	232 ± 19	79.3 ± 8.9	13.4 ± 2.8	4.3 ± 1.5
$W(\ell\nu)$ (EW)	101 ± 15	118 ± 16	135 ± 18	102 ± 13	61.4 ± 7.9	62.2 ± 7.9	39.9 ± 4.8	13.3 ± 1.8	5.6 ± 1.4
Top-quark	206 ± 32	161 ± 25	124 ± 19	60.7 ± 9.3	31.6 ± 6.1	18.3 ± 2.9	11.1 ± 1.8	2.8 ± 0.5	0.9 ± 0.2
Dibosons	219 ± 39	158 ± 28	119 ± 21	50.9 ± 9.1	19.5 ± 3.5	10.4 ± 1.8	2.8 ± 0.5	1.4 ± 0.3	0.4 ± 0.1
Others	77.5 ± 19.5	51.5 ± 11.5	43.8 ± 10.7	14.3 ± 2.9	6.9 ± 1.5	3.7 ± 0.8	2.5 ± 0.6	0.7 ± 0.3	0.3 ± 0.4
Total Bkg.	14960 ± 563	9482 ± 378	6738 ± 281	3032 ± 135	1286 ± 73	849 ± 48	358 ± 28	75.3 ± 9.8	29.9 ± 7.2
Data	16181	10035	7312	3154	1453	919	411	88	29
Signal	591 ± 285	571 ± 232	566 ± 172	472 ± 131	307 ± 64	344 ± 83	228 ± 40	90.3 ± 18.8	37.4 ± 9.1

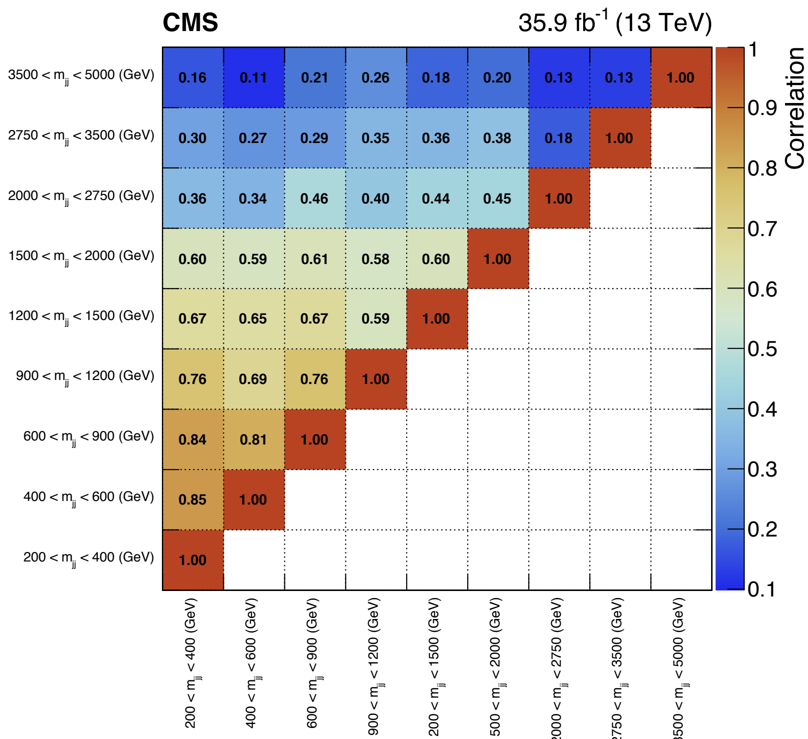

- Data in SR are excluded in the fit assuming the absence of any signal.
- Both can be used in the simplified likelihood approach to reinterpret the analysis results in different models.

Upper Limits on $\mathcal{B}$(H(inv.))

- The observed and expected 95% confidence level upper limits on $\mathcal{B}$(H(inv.)) assuming SM production rate are:

Analysis	Observed limit	Expected limit	±1 s.d.	±2 s.d.	Signal composition
Shape	0.28	0.21	[0.15–0.29]	[0.11–0.39]	52% qqH, 48% ggH
Cut-and-count	0.53	0.27	[0.20–0.38]	[0.15–0.51]	81% qqH, 19% ggH

- Upper limits vs. m_H for SM-like Higgs boson benchmark.

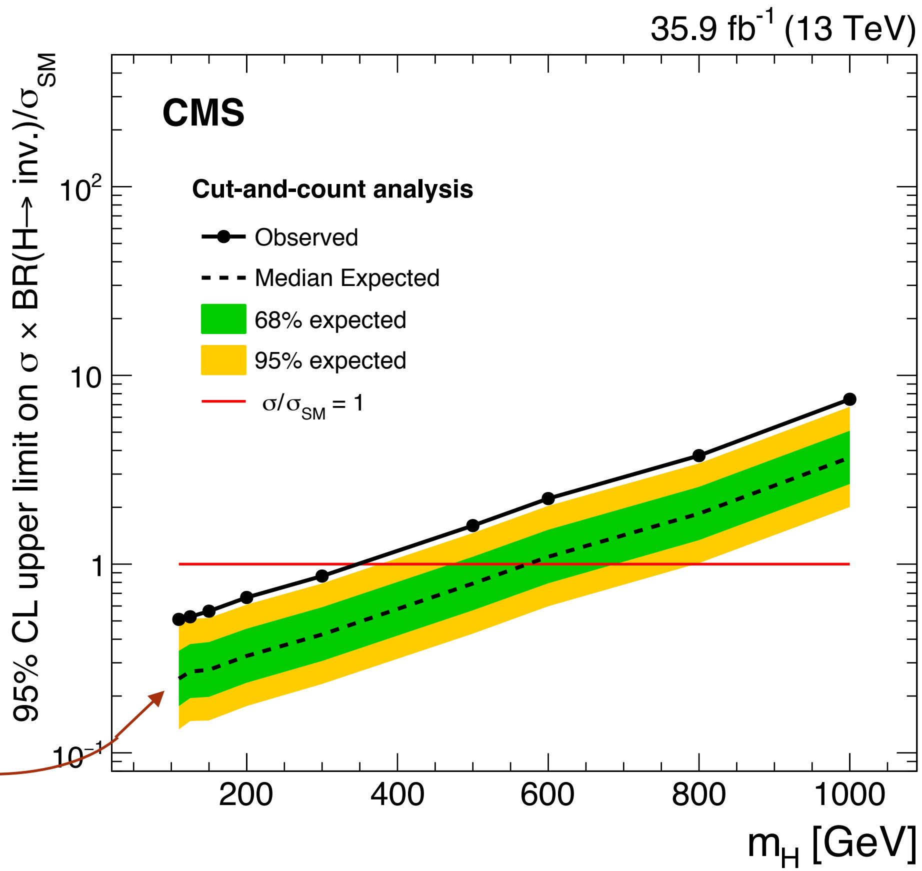

Combination of H(inv.) Searches

- The observed (expected) 95% confidence level upper limits on $\mathcal{B}$(H(inv.)) assuming SM production rate is: **0.24 (0.18)**.

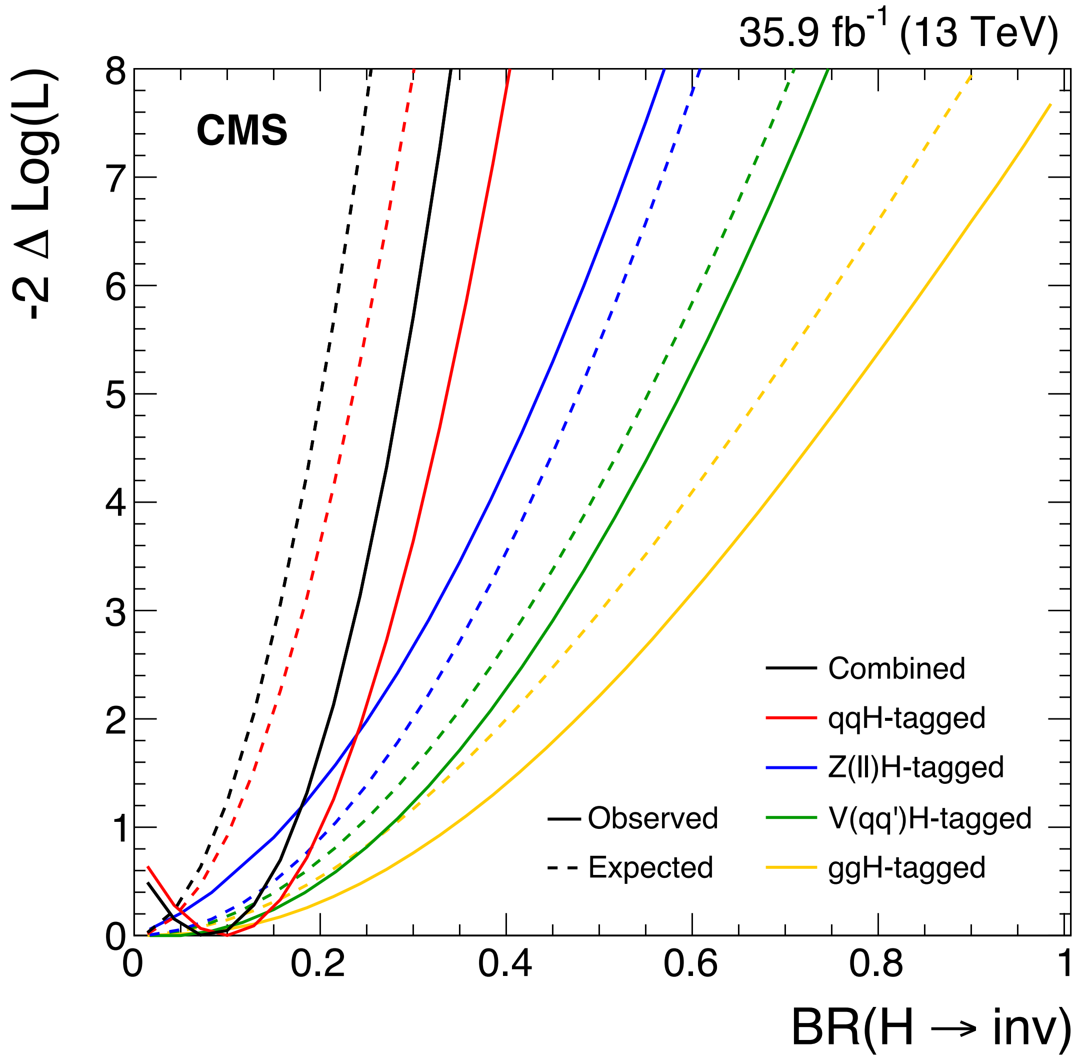

Combination of H(inv.) Searches

- The 95% confidence level upper limit on $\mathcal{B}$(H(inv.)) is expressed as for different assumptions on production (non-SM).
- It shows the result parametrising production cross-sections in terms of coupling strength modifiers, $\boldsymbol{\kappa_F}$ and $\boldsymbol{\kappa_V}$, which scale the coupling of the Higgs boson to SM fermions and vector bosons.
- The 95% confidence level upper limit on $\mathcal{B}$(H(inv.)) varies between 17-29% within LHC couplings constraints.

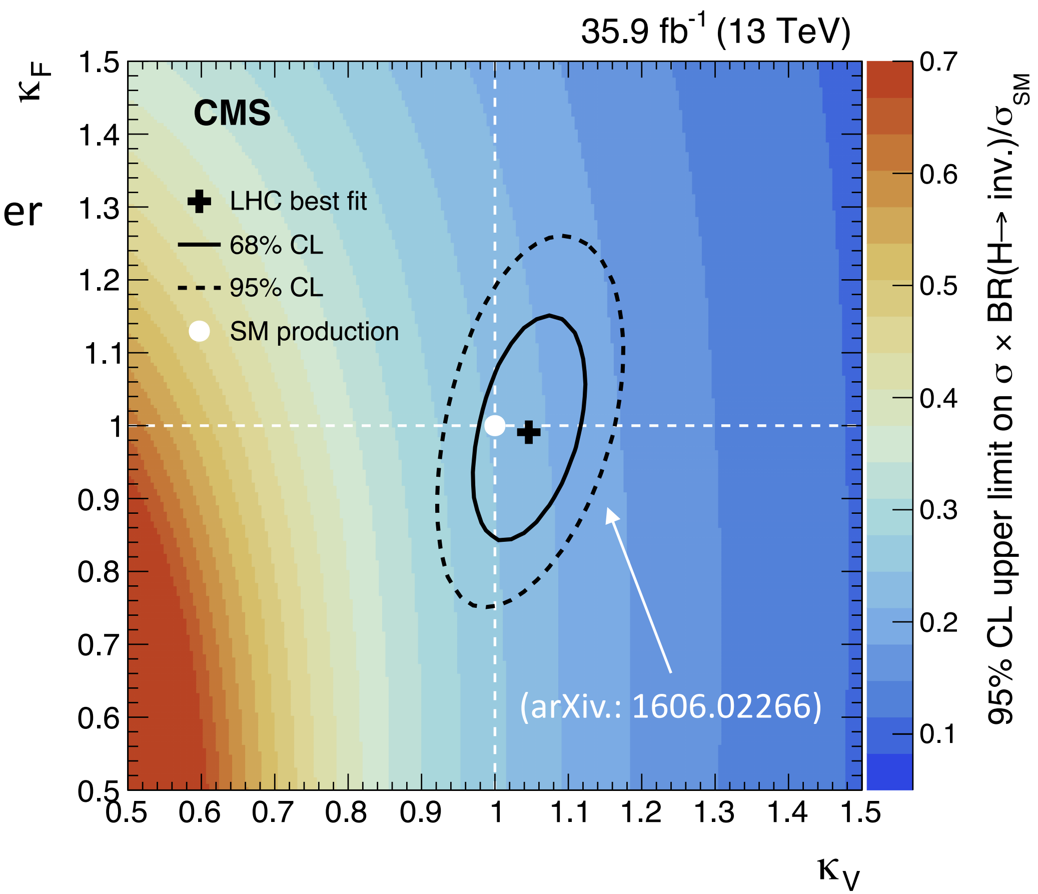

Correlation Scheme

Source of uncertainty	Correlation
Experimental uncertainties	
Luminosity	Correlated across searches
Muon id. eff.	Correlated across searches
Muon reco. eff.	Correlated across searches
Electron id. eff.	Correlated across searches
Electron reco. eff.	Correlated across searches
Muon veto eff.	Correlated across searches
Electron veto eff.	Correlated across searches
B-jet veto eff.	Correlated across searches
Hadronic τ veto eff.	Correlated across searches
Muon energy scale	Correlated across searches
Electron energy scale	Correlated across searches
Jet energy scale	Correlated across ggH, $V(qq')$H and $Z(\ell\ell)$H searches
$p_{\mathrm{T}}^{\mathrm{miss}}$ energy scale	Correlated across ggH, $V(qq')$H and $Z(\ell\ell)$H searches
Muon mis-tag rate	Correlated across single-lepton CR of ggH, $V(qq')$H and qqH searches
Electron mis-tag rate	Correlated across single-lepton CR of ggH, $V(qq')$H and qqH searches
$p_{\mathrm{T}}^{\mathrm{miss}}$ trigger eff.	Correlated across ggH, $V(qq')$H and qqH searches
Electron trigger eff.	Correlated across ggH, $V(qq')$H and qqH searches
Theoretical uncertainties on SM backgrounds	
VV inclusive cross sec.	Correlated across ggH, $V(qq')$H and qqH searches
Top-quark inclusive cross sec.	Correlated across ggH, $V(qq')$H and qqH searches
VV acceptance	Correlated across ggH, $V(qq')$H and qqH searches
Top-quark acceptance	Correlated across ggH, $V(qq')$H and qqH searches
$\mathrm{Z}+\mathrm{jets}/\mathrm{W}+\mathrm{jets}$ ratio vs $p_{\mathrm{T}}^{\mathrm{miss}}$	Correlated between ggH and $V(qq')$H searches
$\mathrm{Z}+\mathrm{jets}/\gamma$+jets ratio vs $p_{\mathrm{T}}^{\mathrm{miss}}$	Correlated between ggH and $V(qq')$H searches
Theoretical uncertainties on Higgs production	
ggH, qqH and VH inclusive cross sec. from QCD-scale	Correlated across searches
ggH, qqH and VH inclusive cross sec. from PDF	Correlated across searches
ggH, qqH and VH acceptance from QCD-scale	Correlated across searches
ggH, qqH and VH acceptance from PDF	Correlated across searches
ggH Higgs p_{T}-dependent unc.	Correlated between ggH and $V(qq')$H searches
VH EWK corrections	Correlated between $V(qq')$H and $Z(\ell\ell)$H searches

DRAFT

CR-only Fit Shape CRs

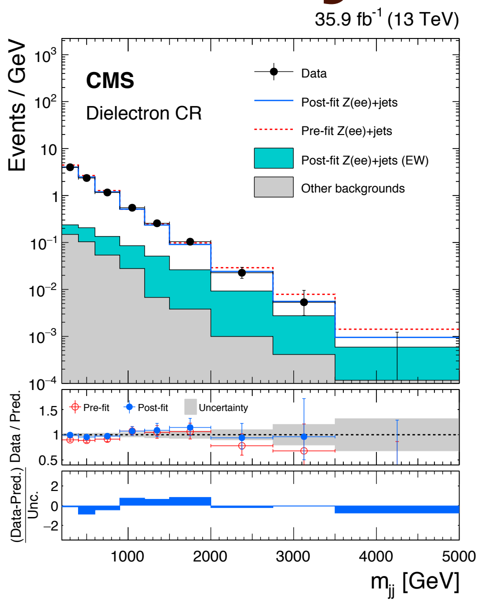

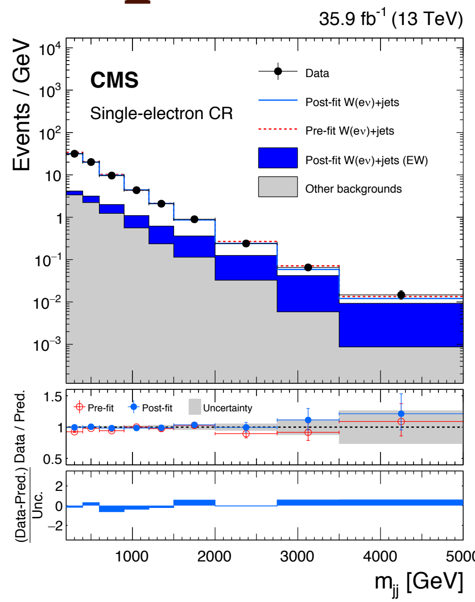

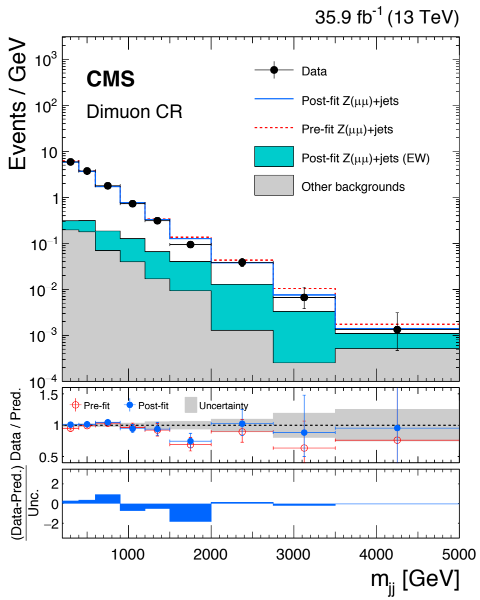

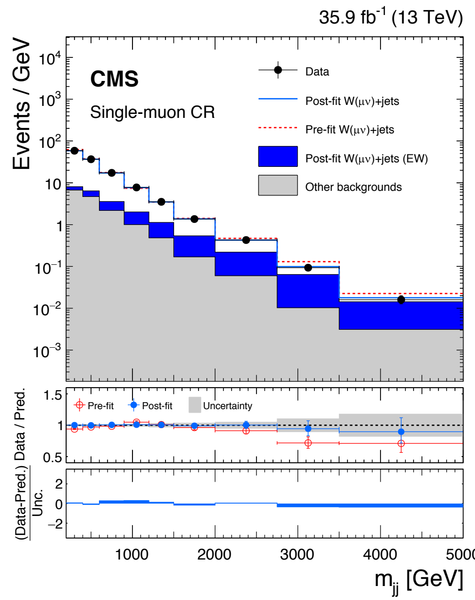

Post-Fit Shape CRs

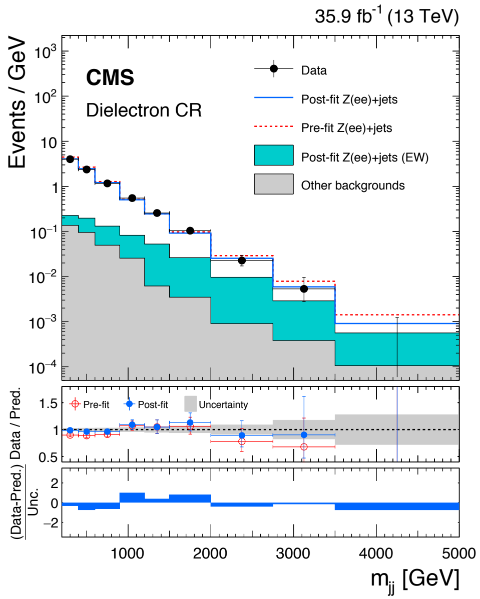

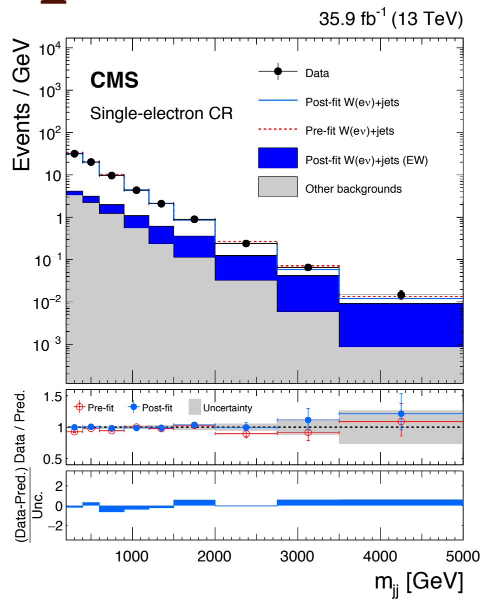

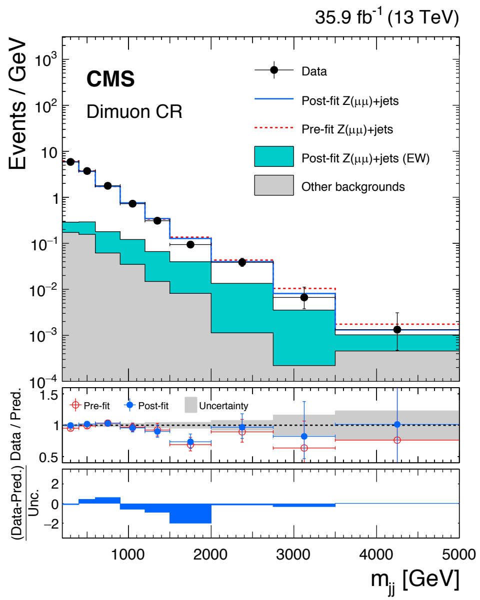

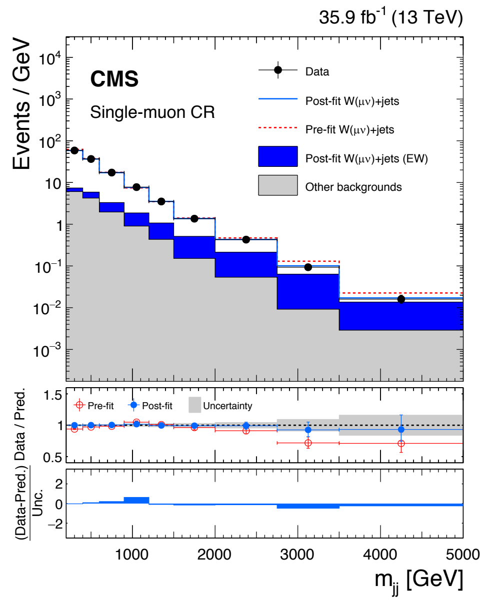

Pre-Fit Shape CRs

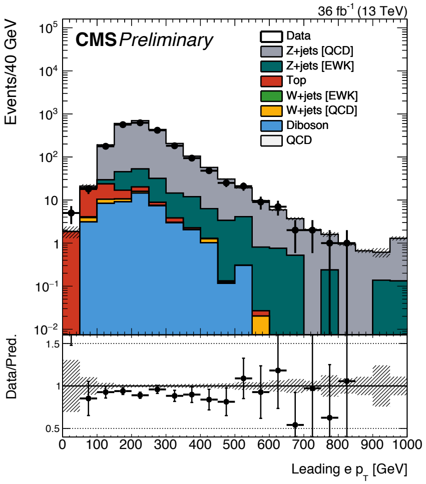

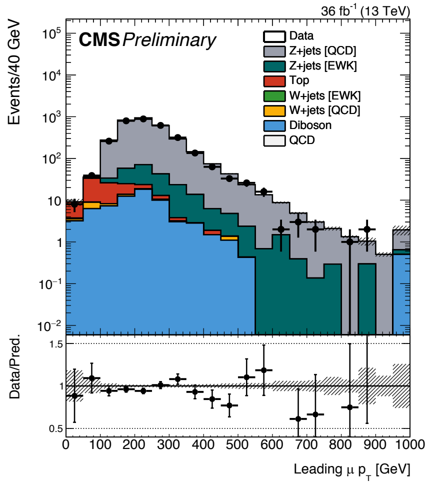

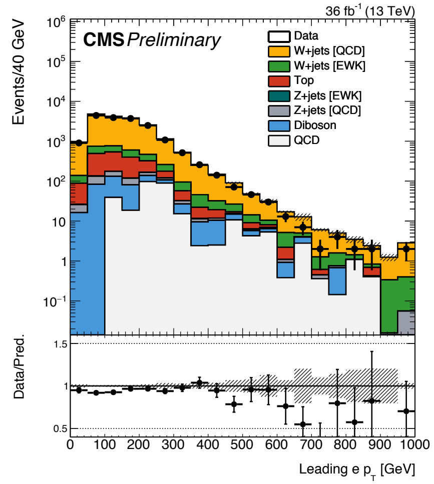

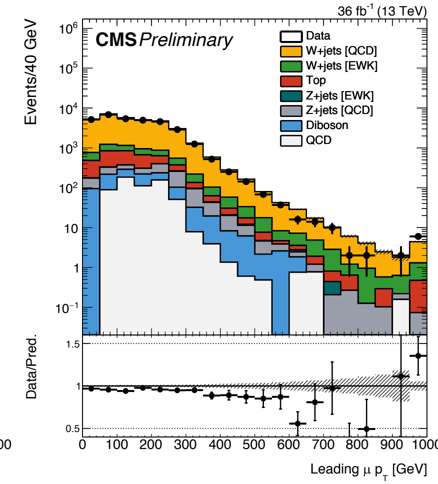

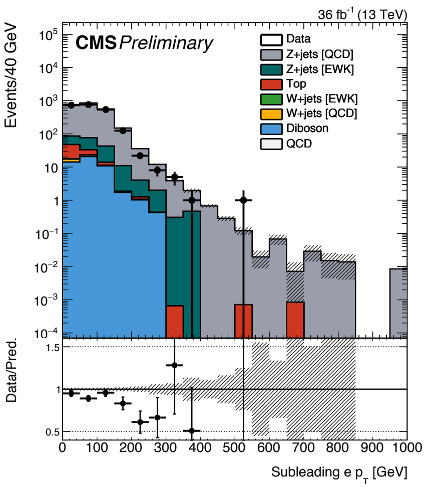

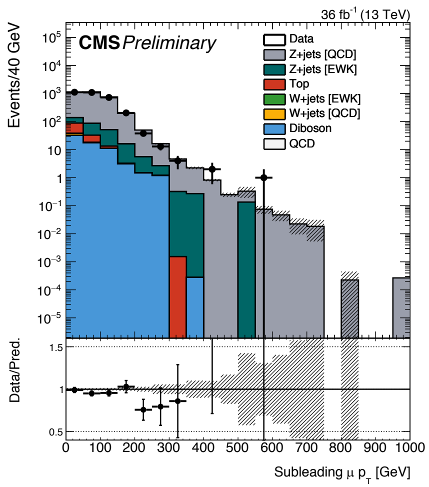

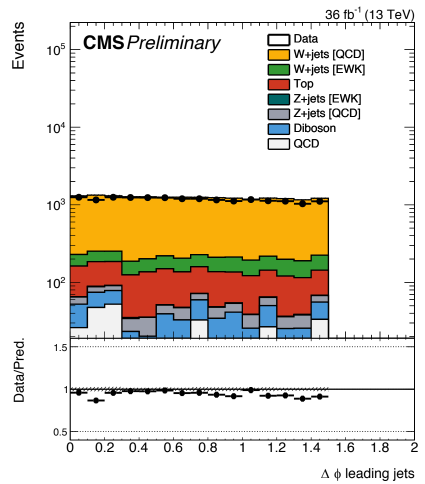

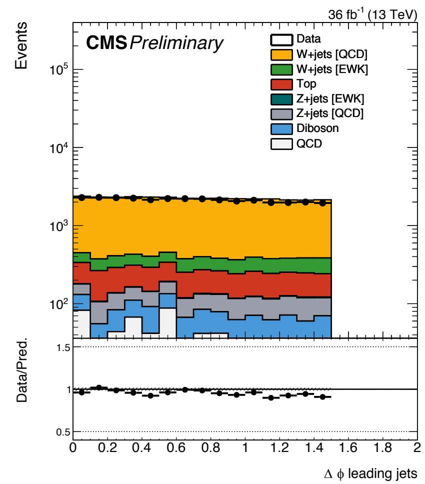

Pre-Fit Shape CRs

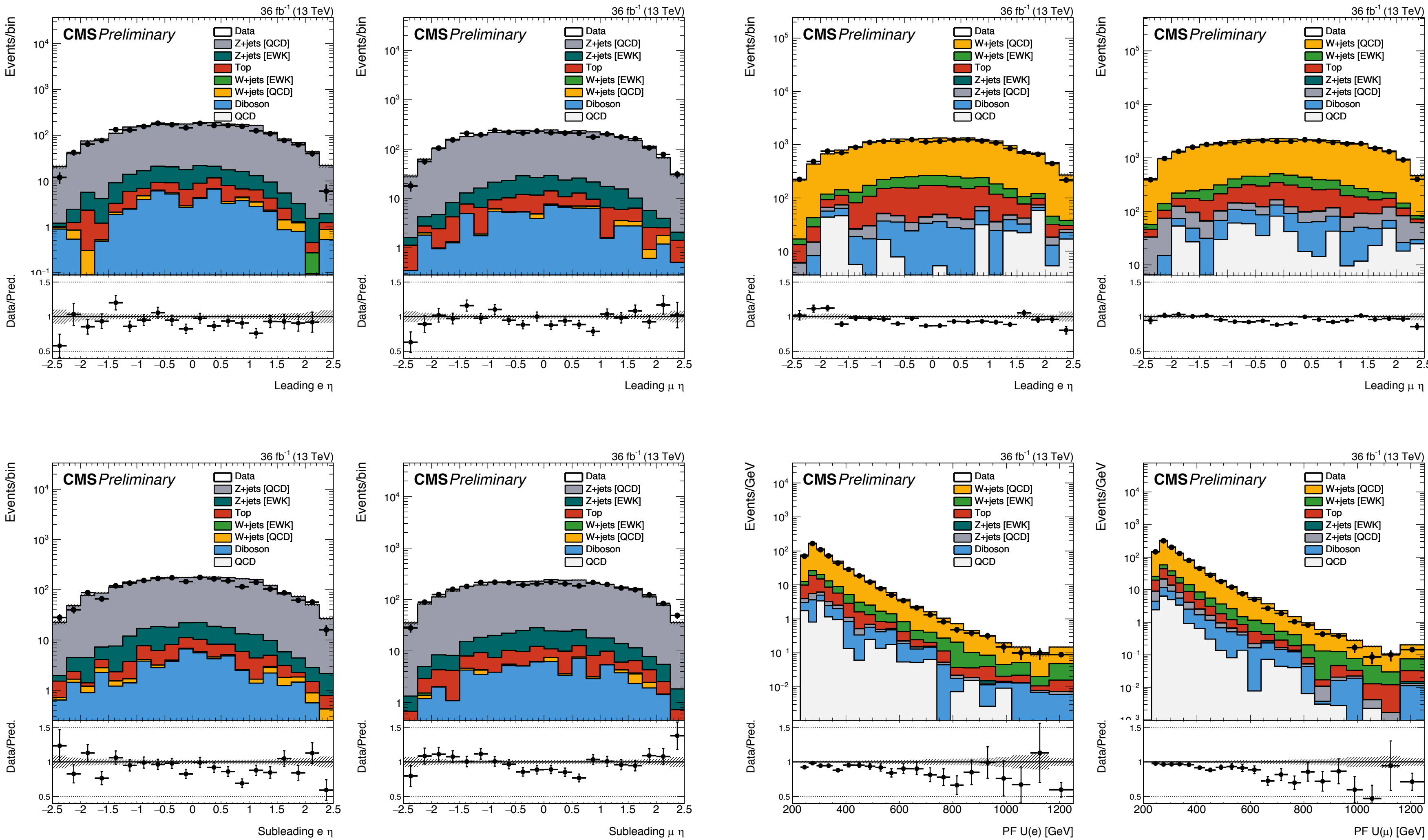

Pre-Fit C&C CRs

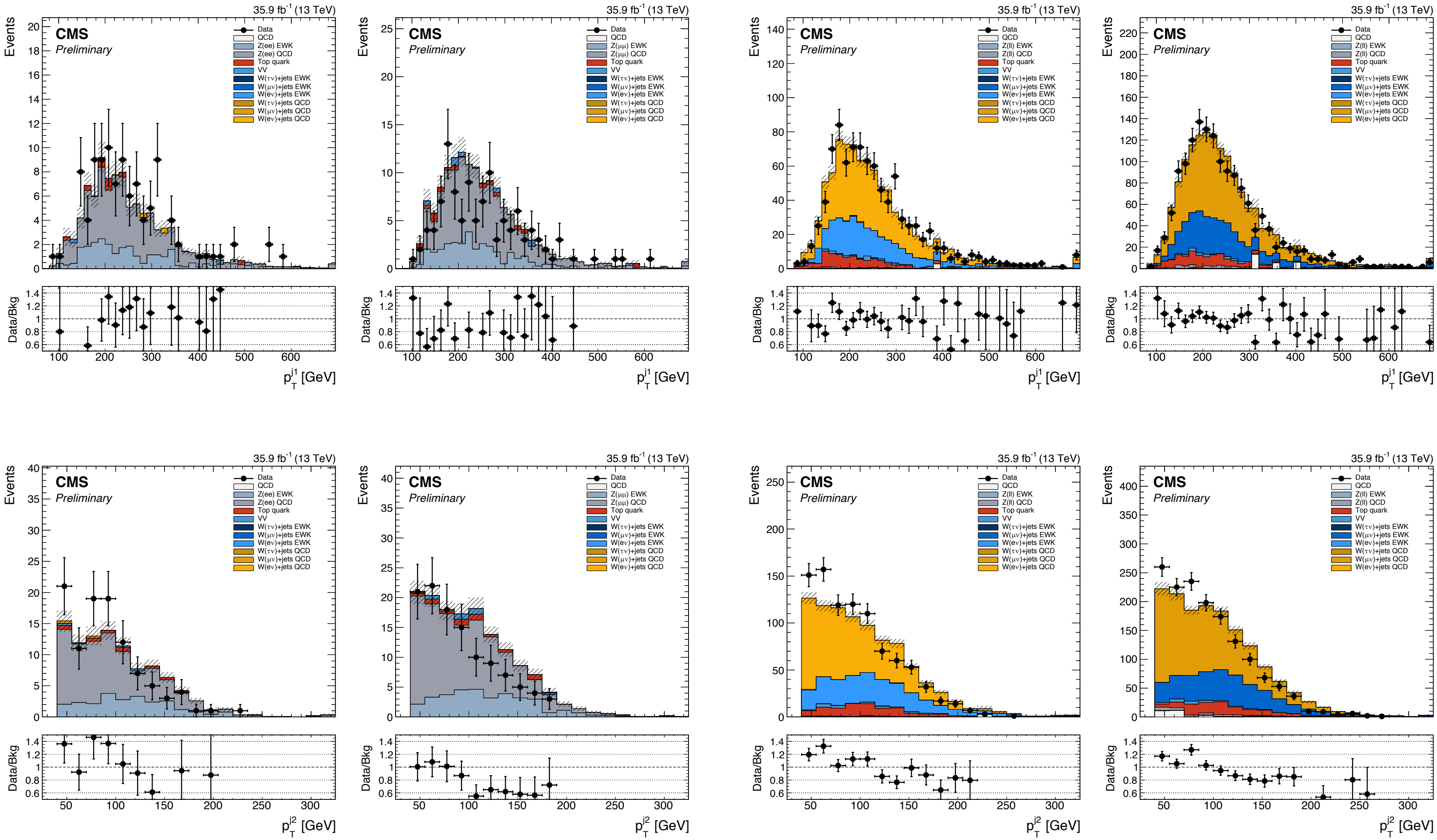

Pre-Fit C&C CRs

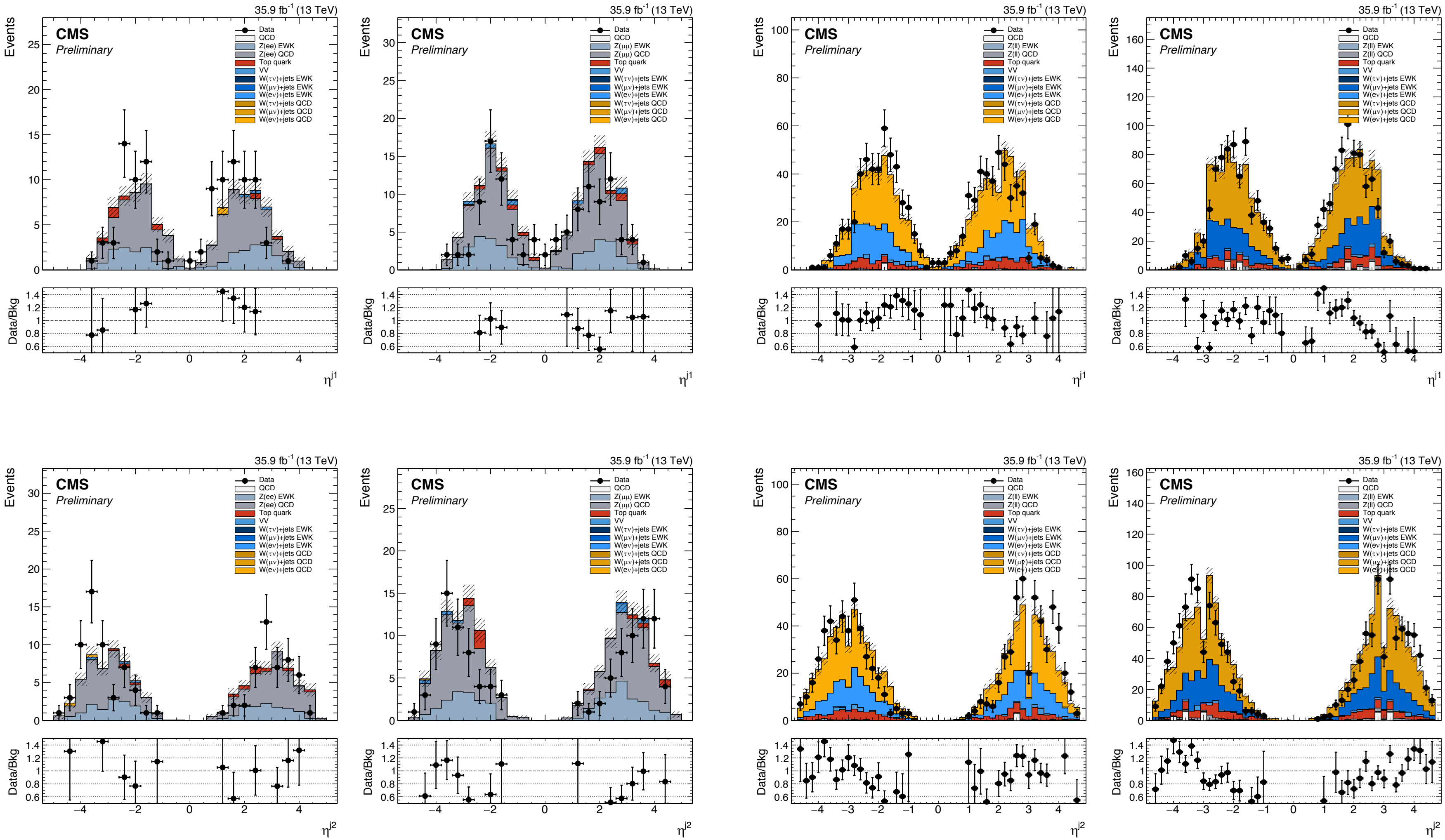

Trigger Efficiency

single-muon

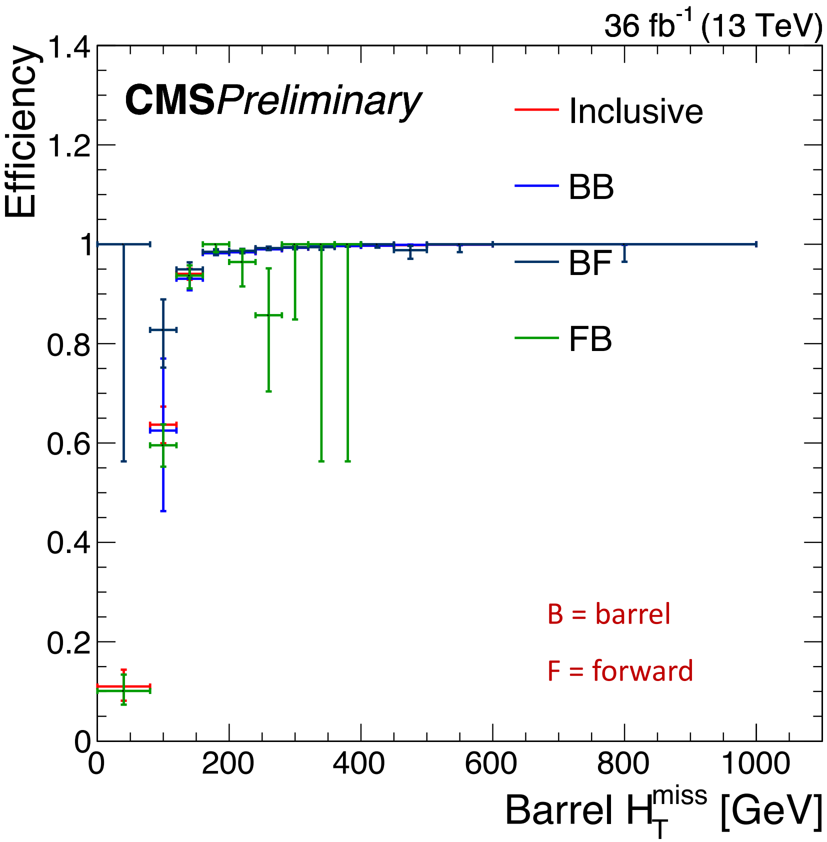

Z tag-n-probe

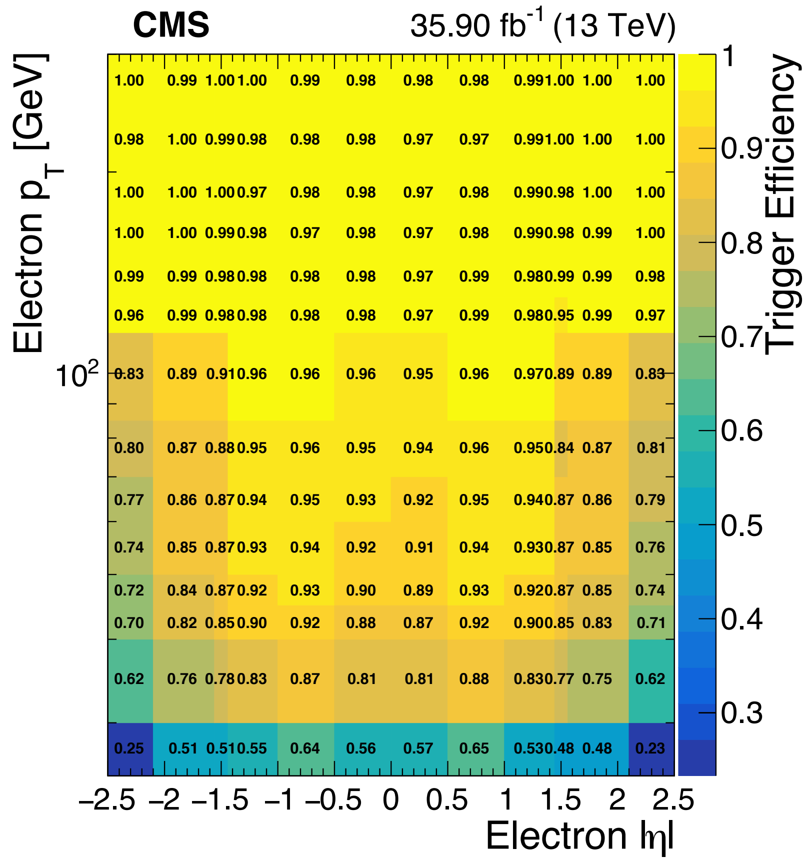

Trigger Efficiency

- We measure the trigger efficiency in W(μν) MC using no reference trigger (i.e. all events that pass the offline criteria) vs. using single-muon reference trigger.

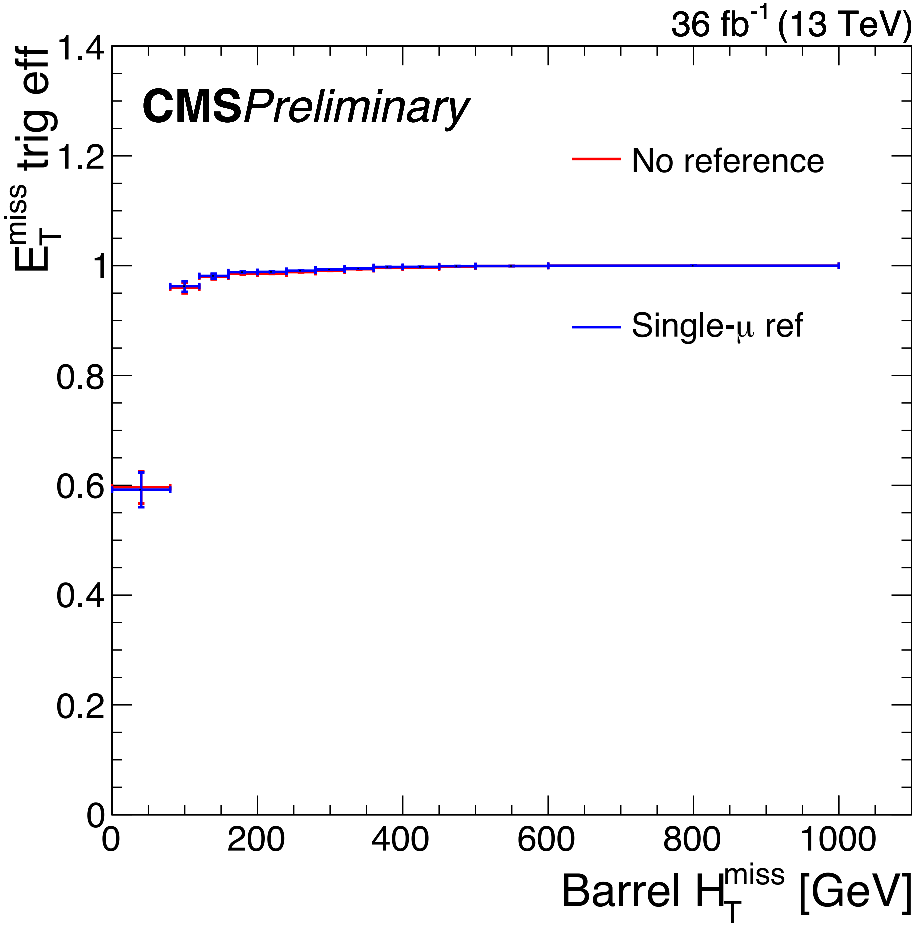

- No bias due to the choice of the reference trigger observed.

Trigger Efficiency

- Simulated efficiencies not used as the emulation of L1 ETM trigger is not very accurate.

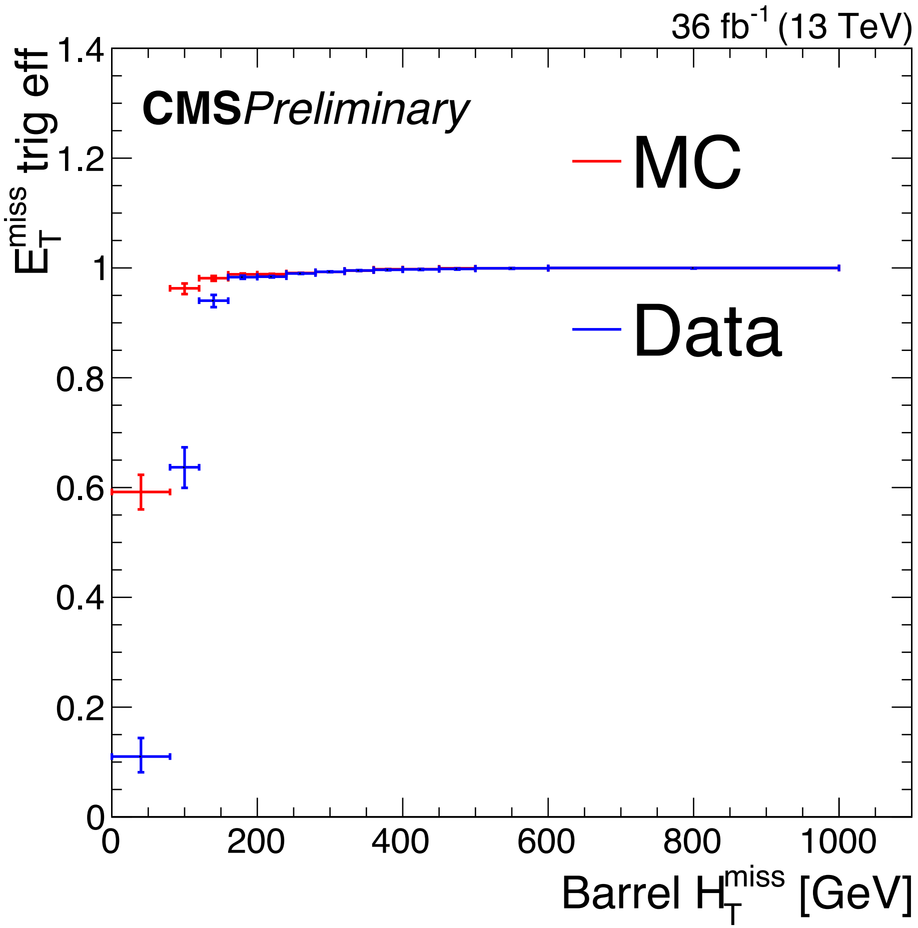

- Good agreement above 250 GeV of threshold.

Trigger Efficiency

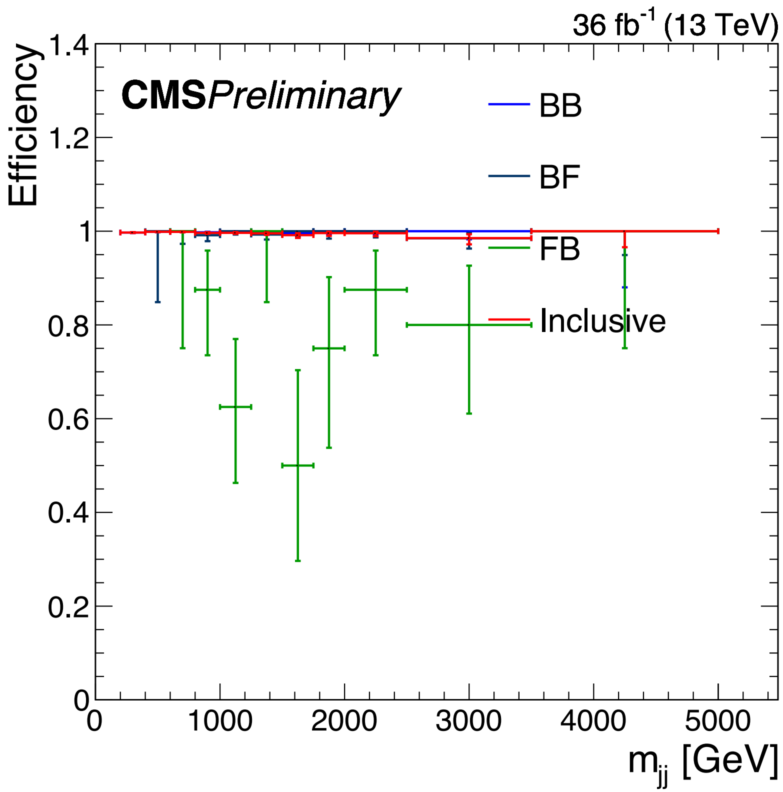

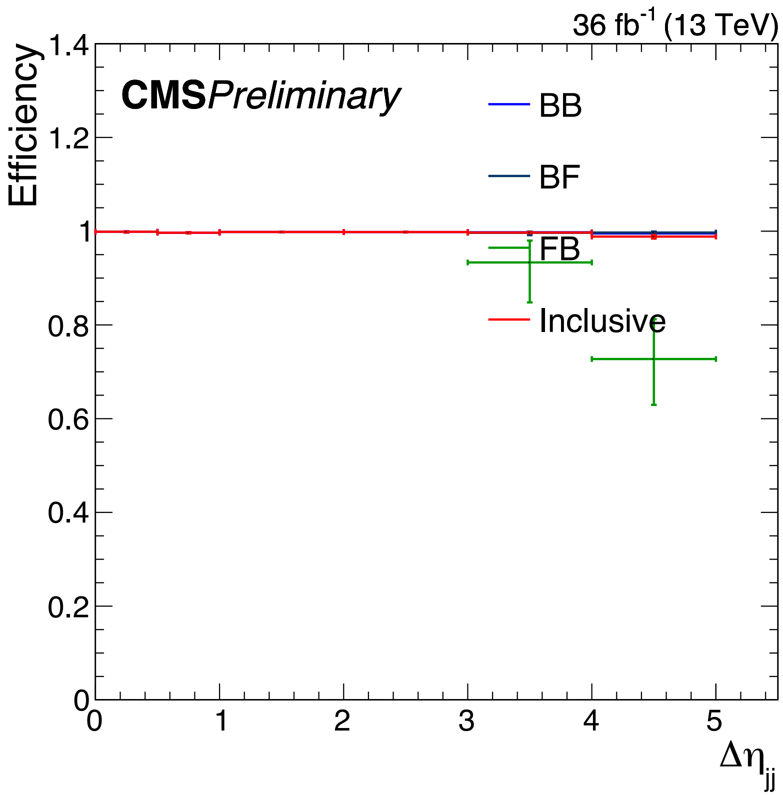

- Inefficiency in the FB category at $\Delta\eta_{jj}$ and m_{jj} is the reflection of the inefficiency seen in the low H_T^{miss} turn-on curves.
- H_T^{miss} observable was chosen as reweighing observable since it was proven to be stable against different inefficiencies based on jet kinematics.

Trigger Efficiency

- To show the sensitivity of the efficiency on PU conditions, we derive the efficiency in a couple of coarse bins based on the number of reconstructed vertices.

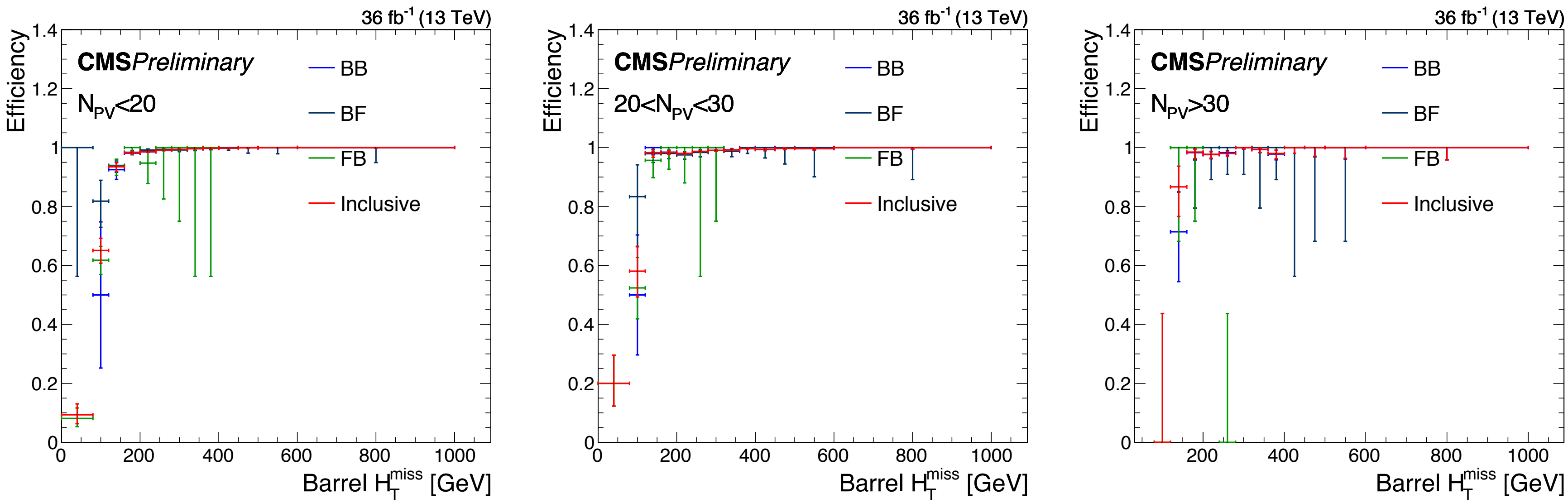

VBF Signal Events

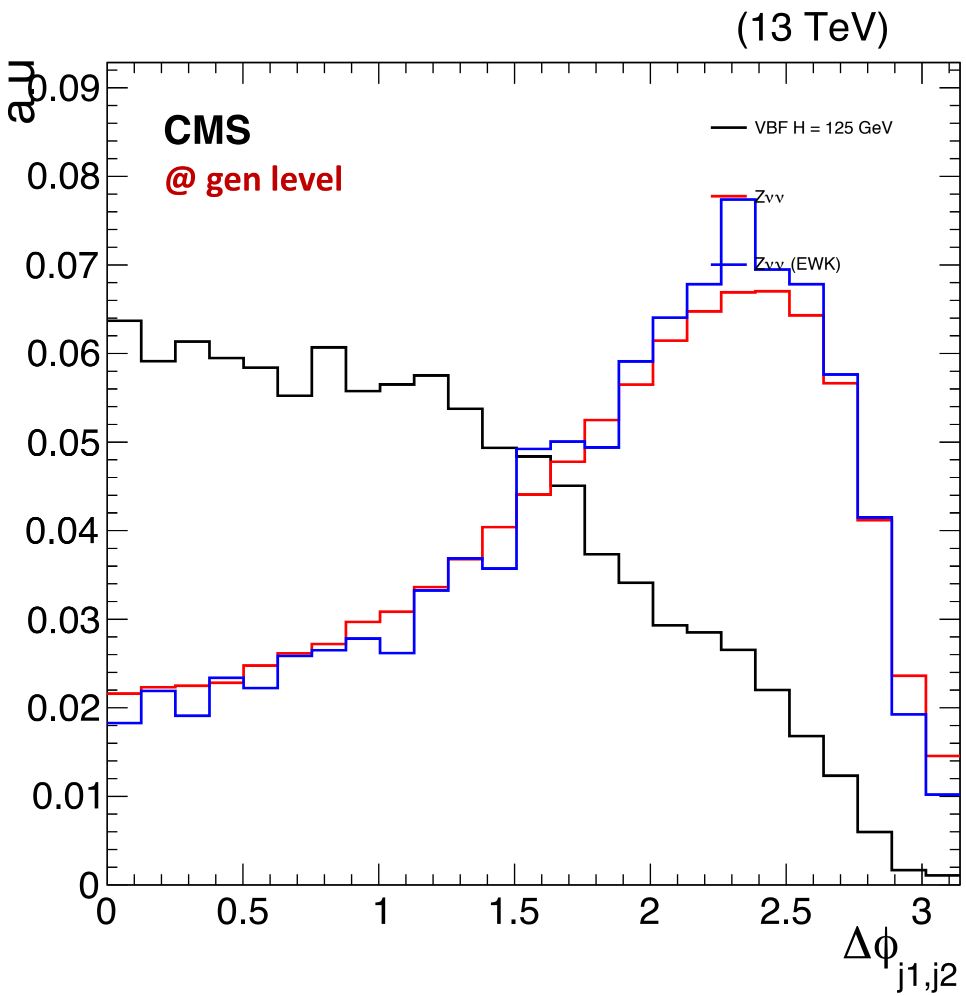

- Small azimuthal separation $|\Delta\phi_{jj}|$ comes from a combination between the J^P properties of the Higgs boson and the high p_T regime explored by this search.

$\mathcal{B}$(H(inv.)) vs. m_H

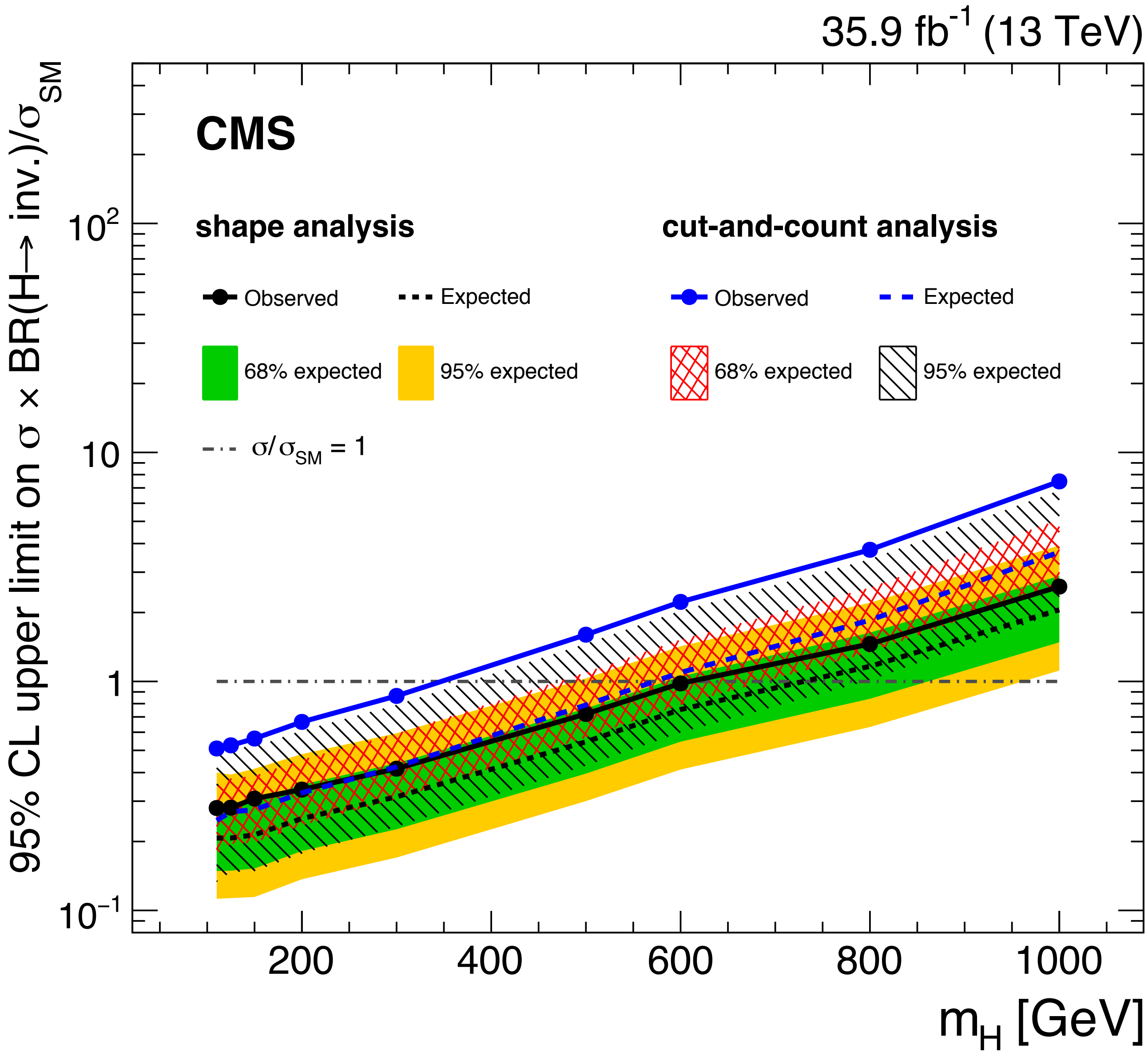

Signal Efficiency vs. m_H

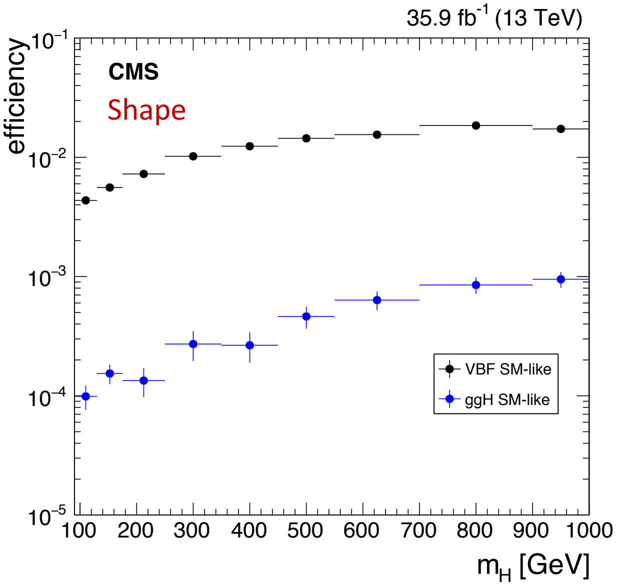

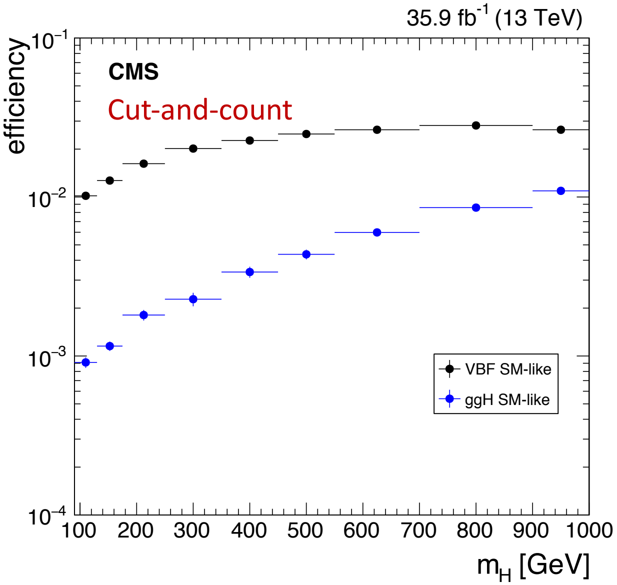

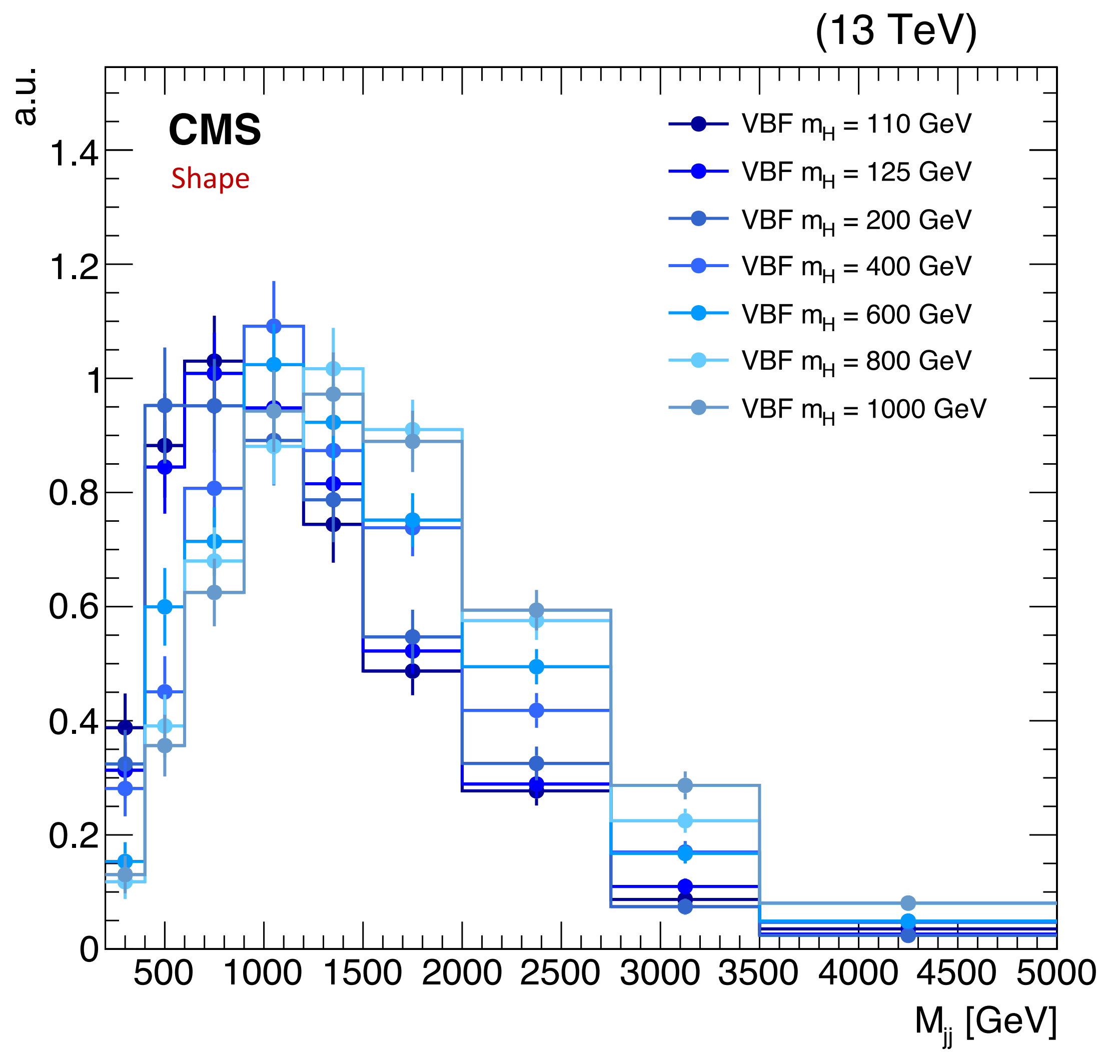

Lepton η distribution discrepancies in CRs

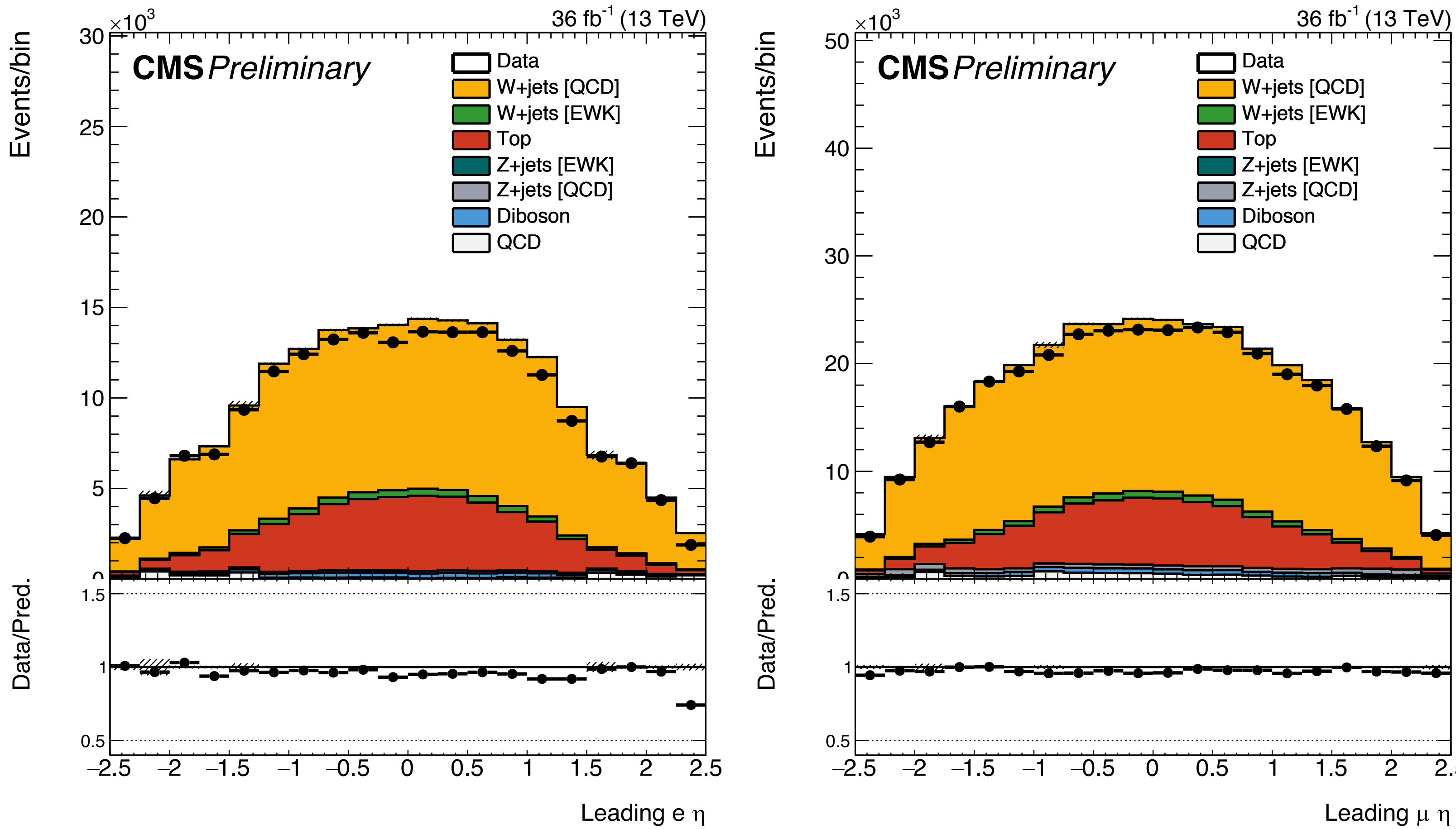

- Disagreement coming from the addition of forward jets (large uncertainties).
- Cross-check: relaxing selection to a mono-jet phase space (single jet in central region), the disagreement is recovered in single-lepton CRs.

Data-MC Disagreement in Trailing Jet p_T

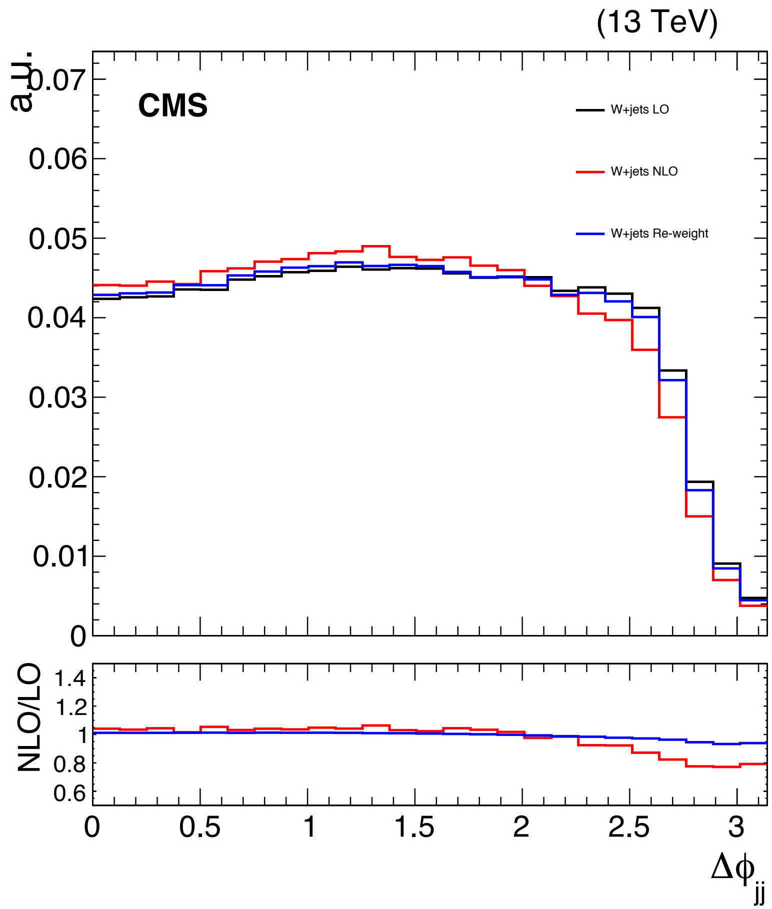

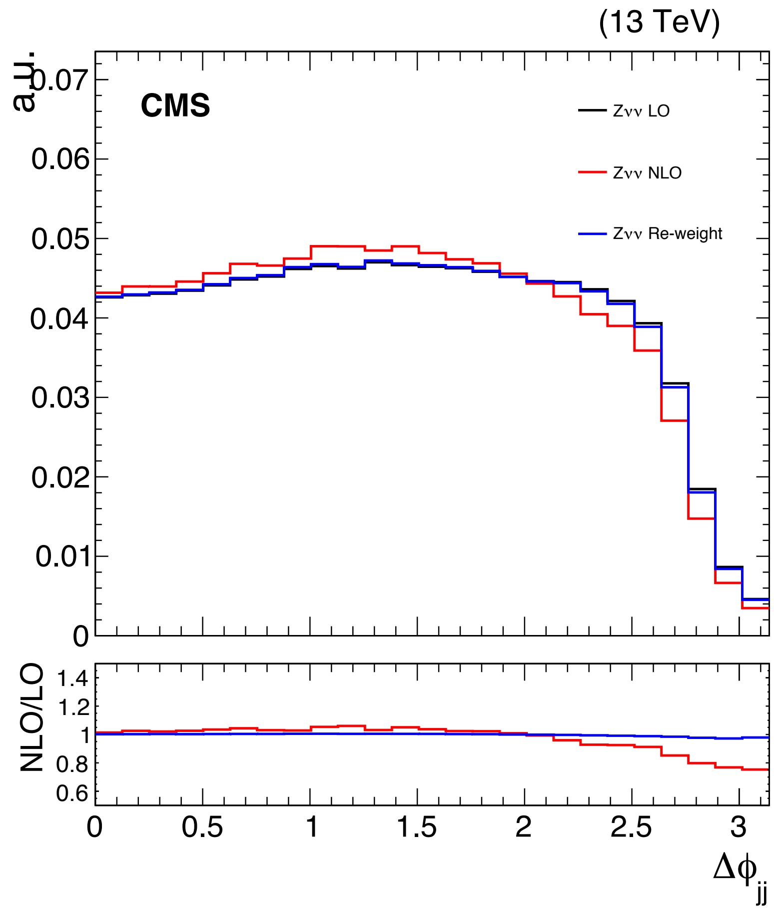

- Comparing shapes between LO V+jets, V+jets + weights (used in the analysis), and NLO V+jets for both Z+jets and W+jets productions, a discrepancy compared to NLO MC is expected, even though we correct the boson p_T and M_{jj} to match higher order predictions.
- The trend is very similar to the one observed in data.

C&C and PU Jet ID

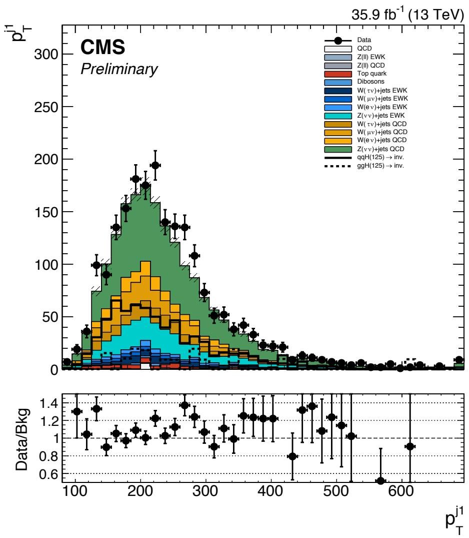

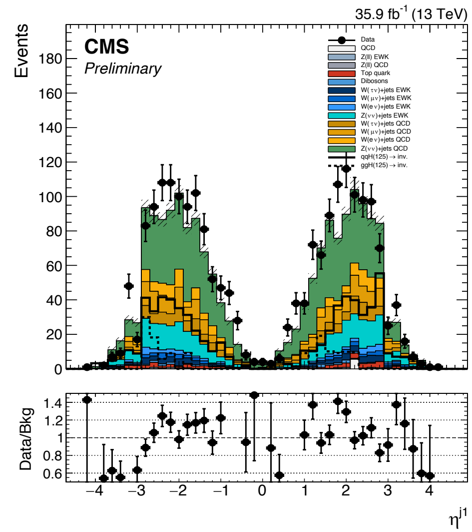

see page 16 at this link

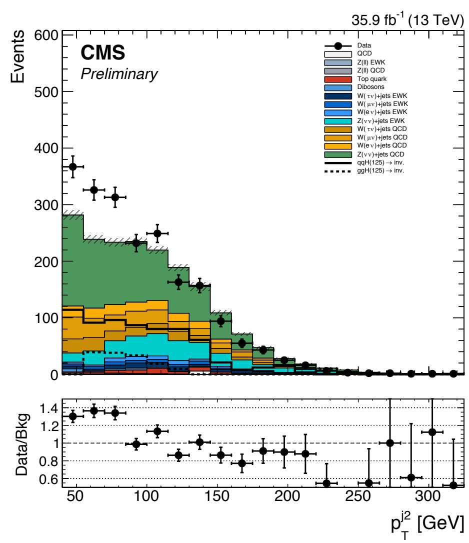

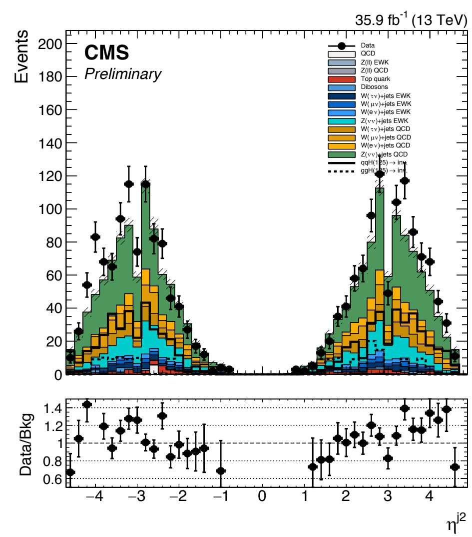

$\Delta\varphi_{jj} \approx 3$ Region in SR

- Shapes of the most relevant kinematic observables compared dividing SR data in 3 exclusive samples: $\Delta\phi_{jj}$ [0,0.2], $\Delta\phi_{jj}$ [0.2,0.5], and $\Delta\phi_{jj}$ [0.5,0.8].
    - ➢ No spikes has been observed in the $\Delta\phi_{jj}$ [0.2,0.5].
- Jet kinematics becomes softer while lowering $\Delta\phi_{jj}$ requirement.
    - ➢ Cross-check: single-muon data events as well as Z(νν) MC confirmed that jets and H_T get softer for events with a small $\Delta\phi_{jj}$.
- Results summarised in the following set of slides [VBF_data_to_data].

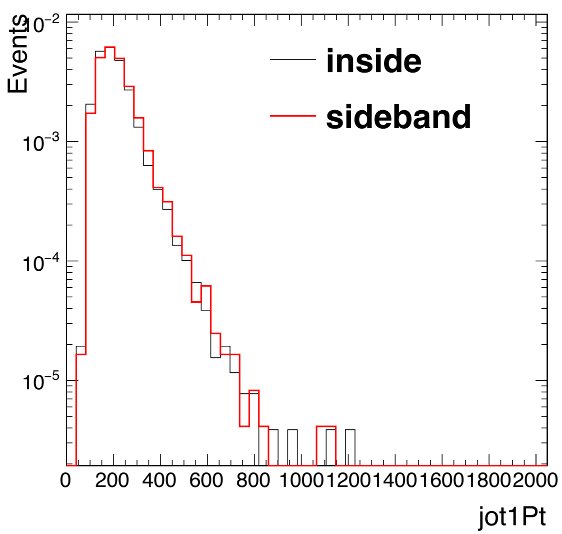

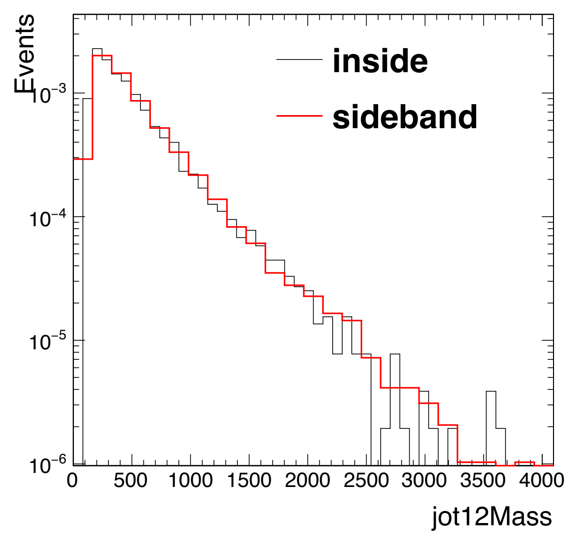

Pre-Fit vs. Post-Fit TFs Comparison

- Pre-fit TFs compared with post-fit TFs, coming from either the CR-only fit or the CRs+SR b-only fit.

  - All the observed trends can be explained in terms of the shift observed in the nuisance parameters (details in ANs).

- Studies summarised in the following set of slides [transfer_factor_comparison].

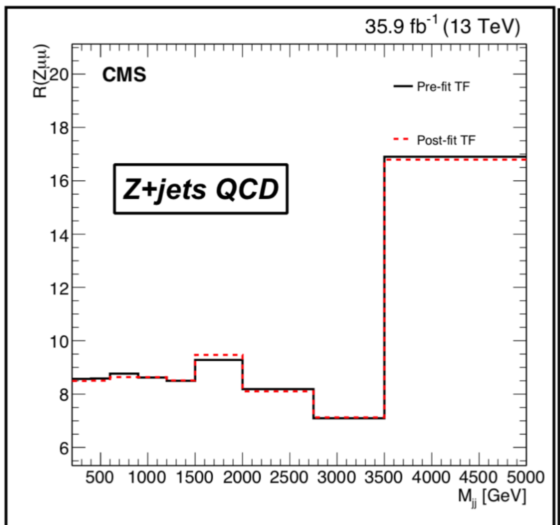

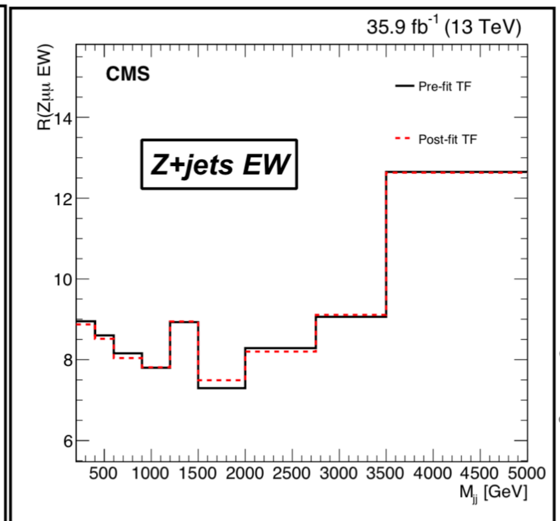

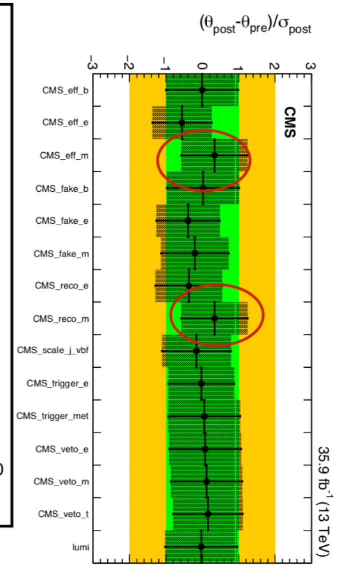

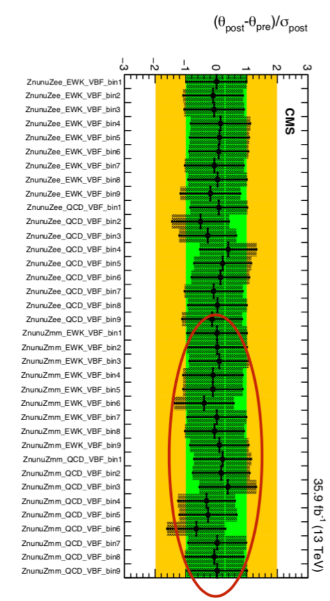

Very small difference between pre-fit and post-fit transfer factors because the Zμμ is the most important CR used to estimate Zνν+jets in the SR. Therefore, the background will be fitted to the data mainly using the freely floating per-bin parameters

Even if muon nuisances are slightly pulled the bin-by-bin uncertainties on the Z/Z ratios are used to compensate for this effect

V+jets Background Estimation

- The fractions of events for W+jets events with one lepton below the p_T threshold are found to be flat across m_{jj}, therefore normalization accounting would be applicable.

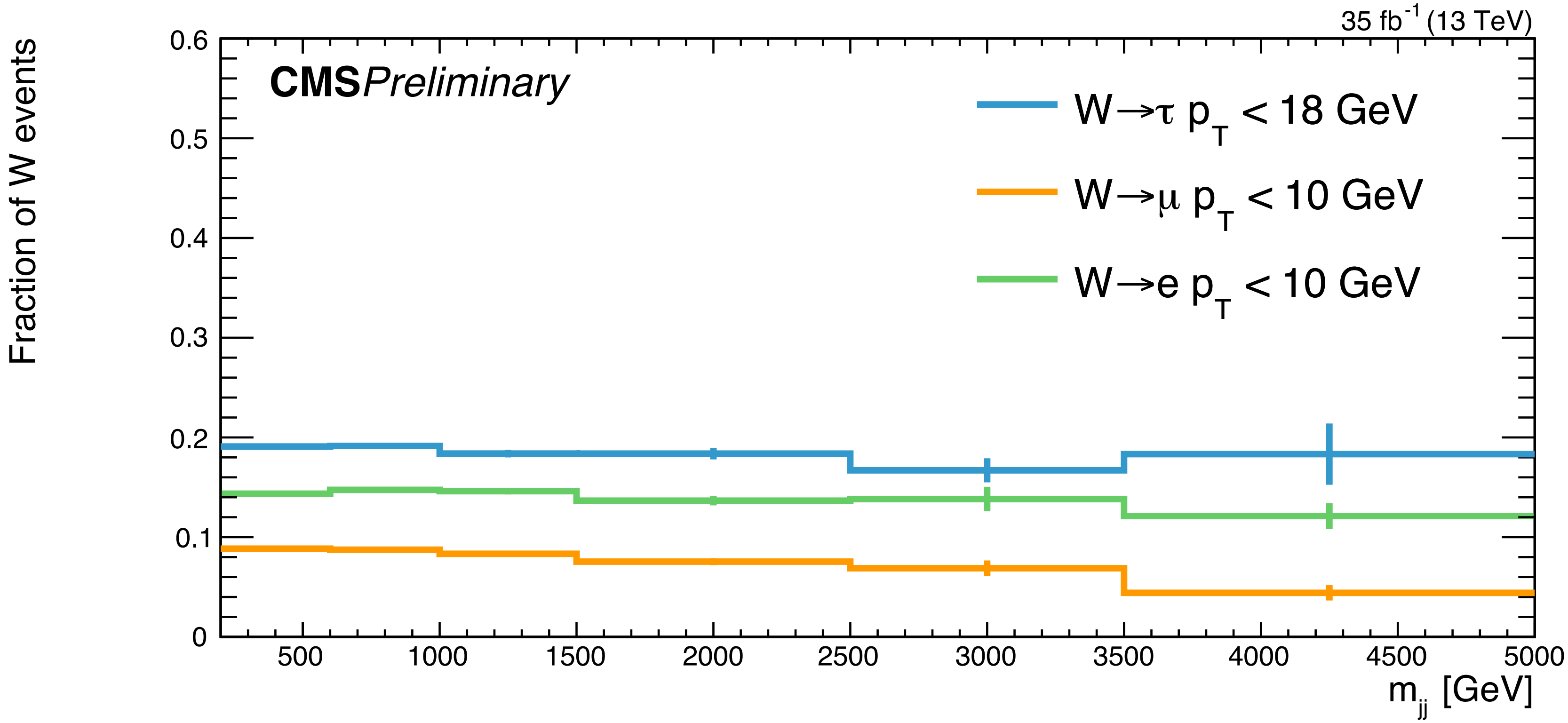

C&C Uncertainty Impact – S+B Fit

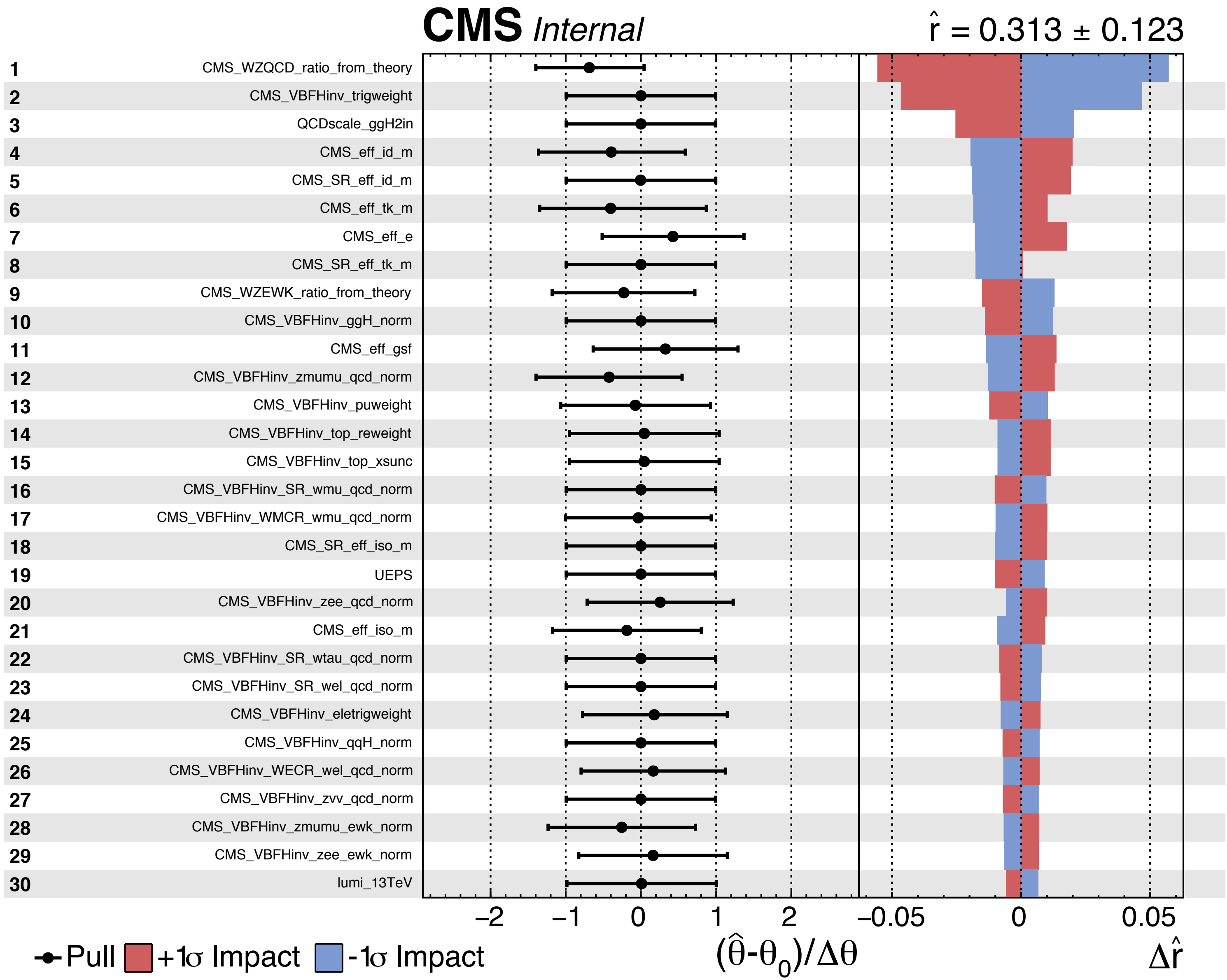

C&C Likelihood Scan

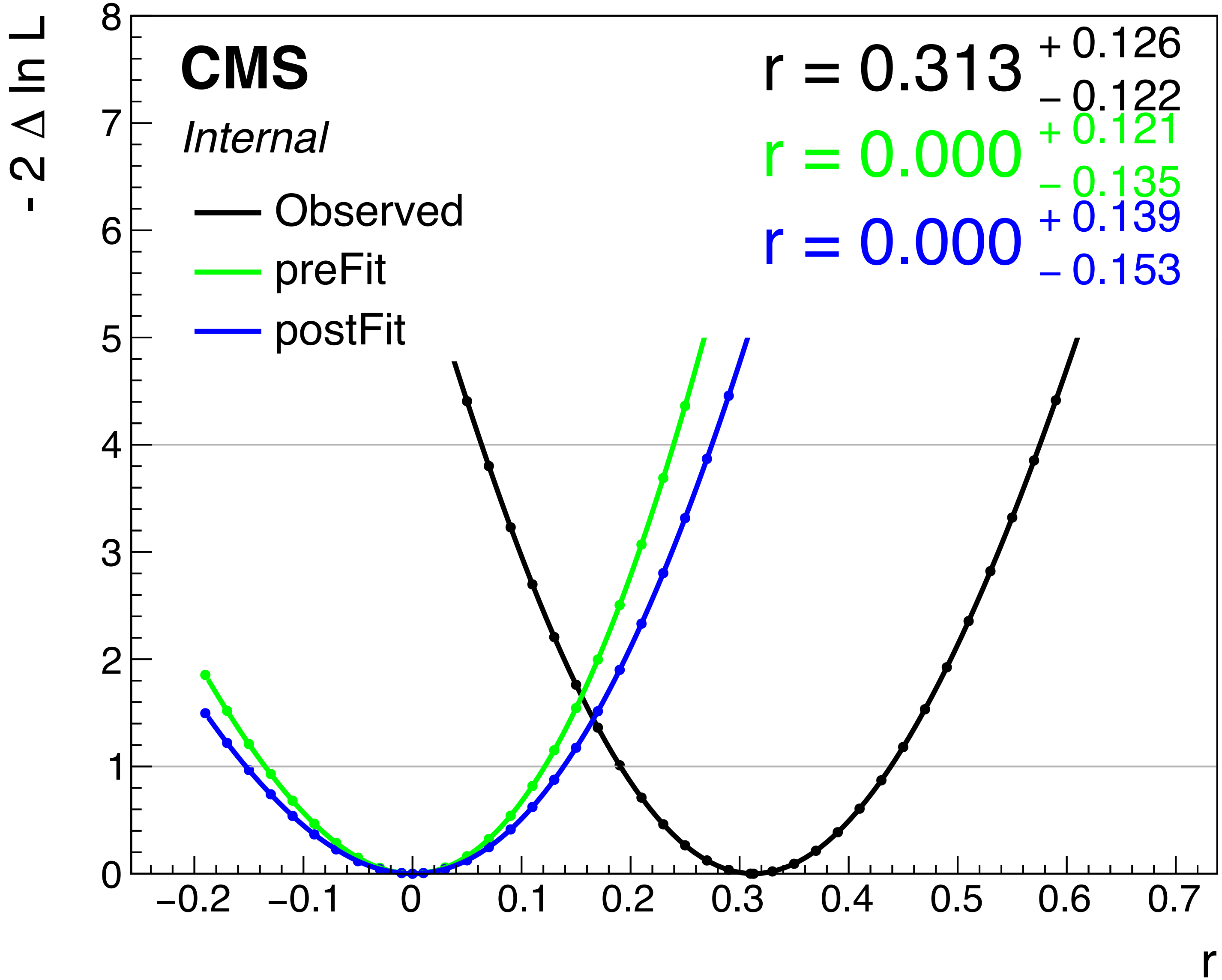

C&C Nuisance Pulls

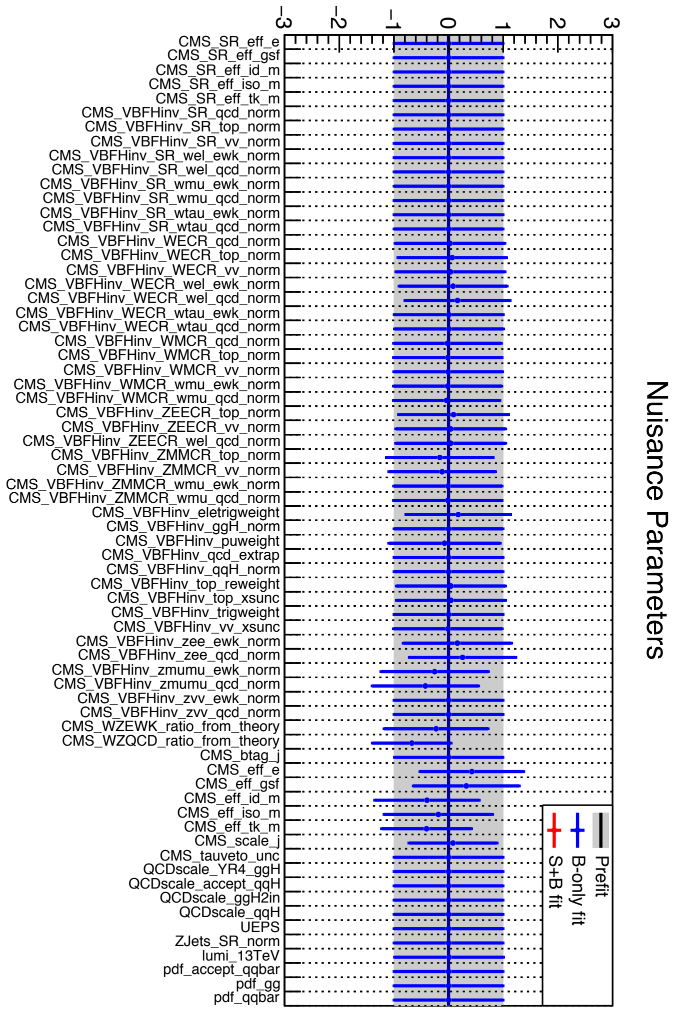

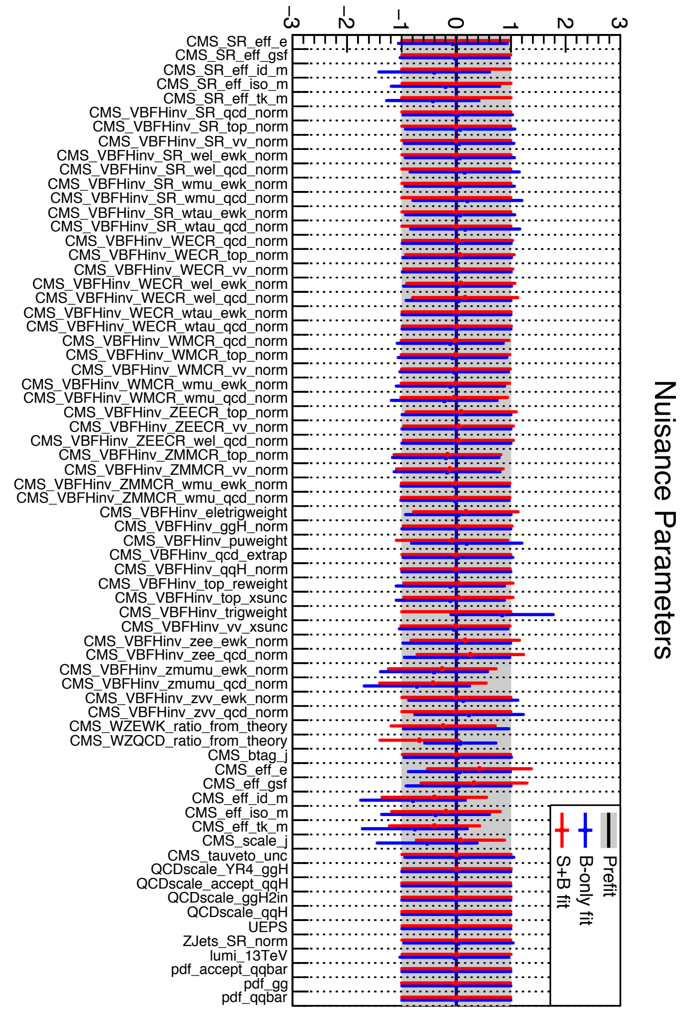

Comparison between CR-only and CRs+SR Backgrounds from B-only Fit and S+B Fit

	Process	Pre-fit (MC)	CR-only Fit	CRs+SR b-only Fit	s+b Fit
Double electron	Top	3.523	3.722 ± 1.111	3.067 ± 0.974	3.714 ± 1.063
	Diboson	0.910	0.944 ± 0.548	0.899 ± 0.514	0.944 ± 0.530
	QCD $W \rightarrow e\nu$+jets	0.790	0.818 ± 0.601	0.827 ± 0.593	0.818 ± 0.435
	EW $Z \rightarrow ee$+jets	25.060	25.004 ± 3.402	26.224 ± 3.485	24.977 ± 3.232
	QCD $Z \rightarrow ee$+jets	68.280	64.752 ± 5.816	72.087 ± 5.586	64.762 ± 6.054
	Observed		104	104	104
Single electron	QCD Multijet	2.871	2.915 ± 2.949	2.992 ± 2.993	2.909 ± 3.137
	Top	80.120	83.029 ± 15.434	71.696 ± 14.021	82.813 ± 15.513
	Diboson	15.570	16.038 ± 4.041	14.666 ± 3.572	16.014 ± 4.208
	EW $W \rightarrow e\nu$+jets	256.900	259.068 ± 10.347	266.159 ± 9.528	259.184 ± 9.710
	QCD $W \rightarrow e\nu$+jets	525.600	531.129 ± 21.212	545.350 ± 19.192	531.319 ± 20.023
	QCD $W \rightarrow \mu\nu$+jets	0.093	0.094 ± 0.003	0.097 ± 0.003	0.094 ± 0.003
	EW $W \rightarrow \tau\nu$+jets	0.673	0.676 ± 0.290	0.701 ± 0.298	0.677 ± 0.308
	QCD $W \rightarrow \tau\nu$+jets	1.875	1.902 ± 0.804	1.926 ± 0.812	1.904 ± 0.795
	EW $Z \rightarrow ll$+jets	2.408	2.428 ± 0.183	2.492 ± 0.183	2.430 ± 0.172
	QCD $Z \rightarrow ll$+jets	4.942	4.964 ± 0.238	5.196 ± 0.229	4.967 ± 0.249
	Observed		914	914	914
Double muon	Top	5.479	5.307 ± 1.622	4.226 ± 1.438	5.289 ± 1.603
	Diboson	2.756	2.622 ± 1.356	2.513 ± 1.191	2.615 ± 1.321
	EW $W \rightarrow \mu\nu$+jets	0.151	0.143 ± 0.151	0.157 ± 0.162	0.143 ± 0.150
	QCD $W \rightarrow \mu\nu$+jets	0.217	0.204 ± 0.222	0.231 ± 0.244	0.203 ± 0.148
	EW $Z \rightarrow \mu\mu$+jets	34.930	32.669 ± 4.344	34.297 ± 4.492	32.630 ± 4.223
	QCD $Z \rightarrow \mu\mu$+jets	101.500	90.031 ± 7.882	100.533 ± 7.185	90.037 ± 7.823
	Observed		114	114	114
Single muon	QCD Multijet	25.410	25.617 ± 20.071	24.237 ± 15.570	25.513 ± 16.718
	Top	125.200	126.599 ± 22.478	108.745 ± 20.585	126.291 ± 22.410
	Diboson	23.670	23.520 ± 4.897	21.948 ± 4.627	23.496 ± 4.823
	EW $W \rightarrow \mu\nu$+jets	421.700	415.708 ± 15.956	427.372 ± 13.821	415.924 ± 14.992
	QCD $W \rightarrow \mu\nu$+jets	904.400	890.997 ± 31.104	915.428 ± 27.641	891.369 ± 30.394
	EW $Z \rightarrow ll$+jets	6.025	5.938 ± 0.292	6.159 ± 0.272	5.942 ± 0.265
	QCD $Z \rightarrow ll$+jets	27.250	26.800 ± 1.191	28.003 ± 1.091	26.816 ± 1.136
	Observed		1512	1512	1512

Comparison between CR-only and CRs+SR Backgrounds from B-only Fit and S+B Fit

	Process	Pre-fit (MC)	CR-only Fit	CRs+SR b-only Fit	s+b Fit
Signal region	QCD Multijet	3.270	3.274 ± 2.658	3.375 ± 2.786	3.274 ± 2.533
	Top	42.790	43.758 ± 9.778	39.274 ± 9.953	43.650 ± 9.744
	Diboson	19.420	19.863 ± 6.094	17.868 ± 5.633	19.825 ± 7.073
	EW $W \rightarrow e\nu$+jets	46.630	46.315 ± 3.570	49.779 ± 3.652	46.351 ± 3.550
	QCD $W \rightarrow e\nu$+jets	133.300	132.393 ± 8.818	142.894 ± 9.020	132.484 ± 9.486
	EW $W \rightarrow \mu\nu$+jets	40.500	40.167 ± 7.922	48.113 ± 8.308	40.204 ± 7.796
	QCD $W \rightarrow \mu\nu$+jets	215.500	213.933 ± 20.061	241.497 ± 18.540	214.086 ± 22.063
	EW $W \rightarrow \tau\nu$+jets	58.830	58.442 ± 3.964	62.748 ± 4.020	58.486 ± 4.336
	QCD $W \rightarrow \tau\nu$+jets	152.300	151.194 ± 9.962	163.312 ± 9.896	151.291 ± 10.667
	EW $Z \rightarrow ll$+jets	0.697	0.695 ± 0.201	0.821 ± 0.217	0.695 ± 0.204
	QCD $Z \rightarrow ll$+jets	8.500	8.434 ± 1.760	9.475 ± 1.862	8.441 ± 1.751
	EW $Z \rightarrow \nu\nu$+jets	284.300	274.758 ± 33.130	302.989 ± 34.530	274.497 ± 33.215
	QCD $Z \rightarrow \nu\nu$+jets	862.500	790.886 ± 66.235	928.114 ± 51.633	791.084 ± 71.234
	Total Background	1868.5	1784.1	2010,3	1784,4
	Observed	XXX	XXX	2053	2053
	gg Higgs (100% $B(H \rightarrow inv)$)	168.500	XXX	XXX	53.404 ± 40.043
	qq Higgs (100% $B(H \rightarrow inv)$)	682.100	XXX	XXX	214.934 ± 88.797

Goodness Of Fit

- Running first on data on CRs and SR:
  - Best fit test statistic: 4.86766 (red line).

- Running then on 500 toy MC datasets to determine the distribution of the goodness of fit indicator:
  - mean expected limit: r < 3.37701 +/- 0.113894 @ 95%CL (500 toyMC) median expected limit: r < 2.69243 @ 95%CL (500 toyMC)
    68% expected band : 1.12946 < r < 5.87749
    95% expected band : 0.367177 < r < 10.4835

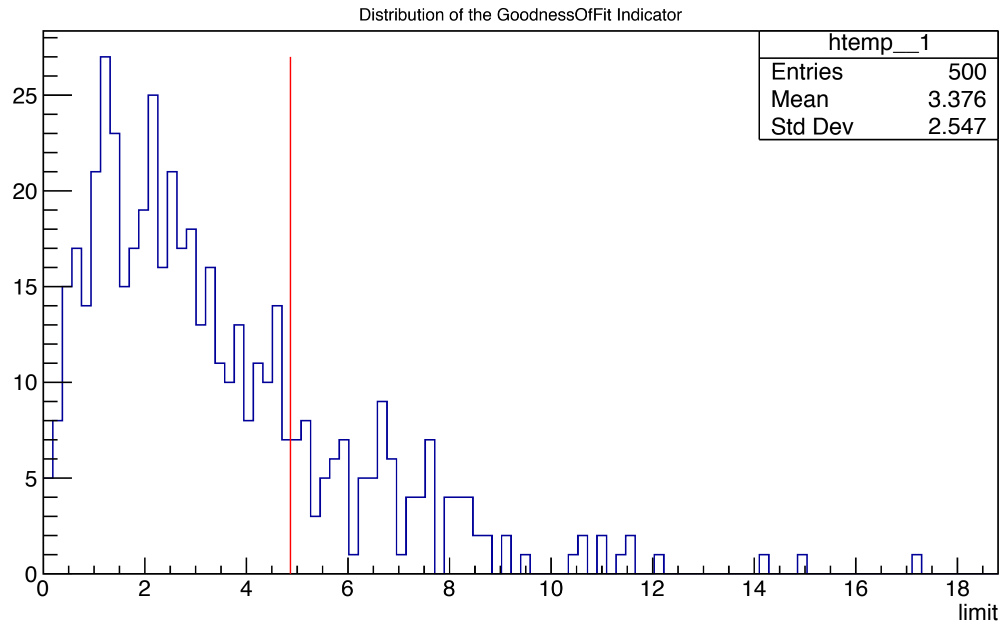

CL_S method

- The limit is computed using the modified frequentist approach CL_s (confidence level) [2,3] based on asymptotic formulas [4,5], exploiting a simultaneous maximum likelihood fit to the signal region as well as the control regions, in which the systematic uncertainties are incorporated as nuisance parameters.

- Perform a single bin counting experiment assuming B(H → inv.) = 100%.

- CL_S statistic is used, which is the number of times more likely the signal hypothesis is than the background hypothesis.

$$CL_s = \frac{P(q_\mu \geqslant q_\mu^{obs} | \mu \cdot s + b)}{P(q_\mu \geqslant q_\mu^{obs} | b)}$$

$$q_\mu = -2 \ln \frac{\mathcal{L}(obs | \mu \cdot s + b, \hat{\theta}_\mu)}{\mathcal{L}(obs | \hat{\mu} \cdot s + b, \hat{\theta})}$$

- Excluding signal models which are less than 5% likely to give data means to exclude everything with $CL_{S+B} < 5\%$.

Feynman diagrams for the combination of H(inv.) searches